ADVANCED SOLAR THERMIONIC GENERATORS

QUARTERLY TECHNICAL PROGRESS REPORT NO. 2
MARCH 1963
AF 33(657)-8947

Aeronautical Systems Division
Air Force Systems Command
United States Air Force
Wright-Patterson Air Force Base, Ohio

GENERAL ELECTRIC
MISSILE AND SPACE DIVISION

ADVANCED SOLAR THERMIONIC GENERATORS

QUARTERLY TECHNICAL PROGRESS REPORT NO. 2
MARCH 1963
AF 33(657)-8947

Aeronautical Systems Division
Air Force Systems Command
United States Air Force
Wright-Patterson Air Force Base, Ohio

AUTHORS: R. R. Herrick,
R. C. Keyser
L. L. Dutram

Project Engineer: R.R. Herrick

Approved By: Dr. J. C. Danko, Manager
Advanced Space Power Engineering

GENERAL ELECTRIC
MISSILE AND SPACE DIVISION
Valley Forge Space Technology Center
P.O. Box 8555 • Philadelphia 1, Penna

The work covered by this report was accomplished under Air Force Contract AF 33(657)-8947, but this report is being published and distributed prior to Air Force review. The publication of this report, therefore, does not constitute approval by the Air Force of the findings or conclusions contained herein. It is published for the exchange and stimulation of ideas.

FOREWORD

This report covers work completed during December, January, and February of 1963; by the General Electric Company, Missile and Space Division, Spacecraft Department at Philadelphia, Pa. on Air Force Contract No. AF 33(657)-8947, Project No. 8173, Task No. 817305-16, "Advanced Solar Thermionic Generators." The work was administered under the guidance of A. E. Wallis, Flight Accessories Laboratory, Aeronautical Systems Division.

General Electric personnel who actively participated in this work are:

Name	Area of Responsibility
R. R. Herrick	Project Engineer
L. L. Dutram	Engineer, Converter Design & Integration
R. C. Keyser	Engineer, Generator Design & Test
J. F. Williams	Technician, Thermionic Systems
D. L. Purdy	Consulting Engineer, Thermionic Systems
Dr. J. M. Houston	Consultant, Thermionics (General Electric Research Laboratory)
Dr. J. C. Danko	Manager, Advanced Space Power Engineering

TABLE OF CONTENTS

LIST OF ILLUSTRATIONS

ABSTRACT

Designs and analyses for the STEPS III converters and generator are presented.

Performance expected from the converters and from the system in solar operation is estimated.

Test results are given for preliminary converters used to evaluate spacing techniques and cathode materials.

1.0 CONVERTER DESIGN AND ANALYSIS

1.1 Converter Design Concept

The design of converters for use in the STEPS III "integral generator" has been based on three objectives:

1) Advance the state-of-the-art toward higher converter efficiencies and greater power densities, such as would be applicable for flyable systems.

2) Provide a long life design of high reliability.

3) Produce converters suitable for generator testing which are reproducible and can be used as test devices to compare variables such as spacing and cathode-anode material combinations.

In addition, the design was based on mechanical configurations that had been previously proven in designs fabricated and tested by the General Electric Research Laboratory and Power Tube Department. Converters have been designed to use cathode materials of rhenium or tantalum and anode materials of rhenium, tantalum or molybdenum. This analysis of converter performance is given for an emission level as represented, for example, by reported data on rhenium-molybdenum. The analysis applies to any material combination with this emission level.

In the STEPS III Program the converters will first be used to test and evaluate a variety of cathode-anode materials for specified periods of converter life. In order to provide consistent test data, the converter must be able to operate with a fixed spacing which may be reproduced from tube to tube in order to remove spacing as a variable from the test results. In order to accomplish fixed spacing, a system of tungsten pins, a tungsten tensile rod and an envelope bellows section have been introduced into the design which provides reproducibility in spacing with variations less than 0.0002 inches from tube to tube. This spacing mechanism should prove constant with time and temperature.

While providing a mechanism for comparison of test results, the tube configuration also will provide a cool seal region, which, coupled with the invariant spacing, should prolong tube life by removing structural problem areas.

The design of the tube has incorporated the highest reported emission data, and cathode temperatures in the 1750°K to 1950°K range. Operation at other cathode temperatures may then be optimized by suitable radiation shielding of the anode fin to provide optimum fin temperatures over the desired range of cathode temperatures.

Figure 1 shows the final C Series converter design. Parts 4, 13 and 18 in Figure 1 illustrate the pin spacers, tensile rod and spring, respectively.

1.2 Anode Temperature Selection

The anode temperature has been selected on the basis of data obtained at the General Electric Research Laboratory on planar converters, published in Reference 3, and plotted in Figure 2. The converter size was selected to achieve the optimum anode temperature at peak power operation and will run considerably cooler at other operating points. Optimized anode temperature may then be achieved by varying anode radiator shielding to increase the fin temperature, thus increasing the temperature of the anode. From Figure 2, the optimum anode temperature is 1030°K at 1950°K cathode temperature.

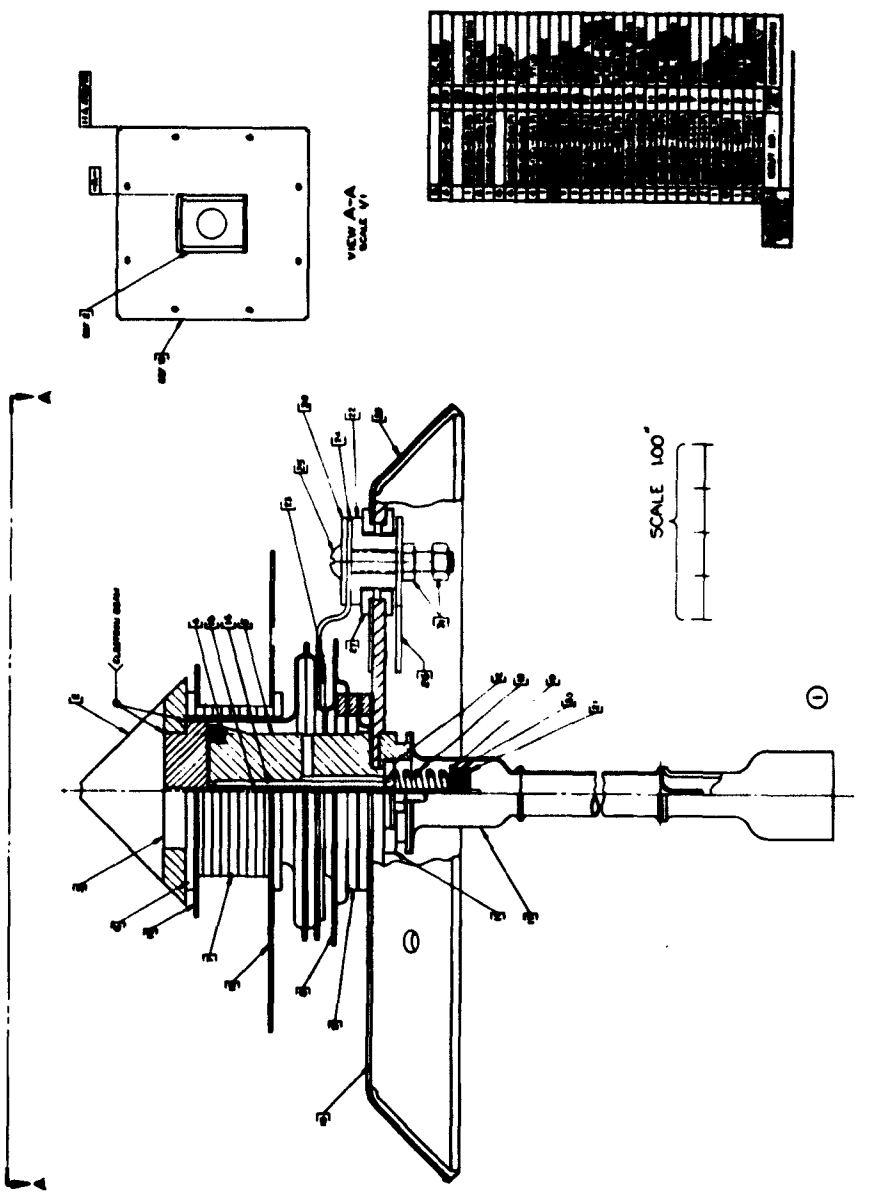

Figure 1. STEPS III C-Series Converter Assembly

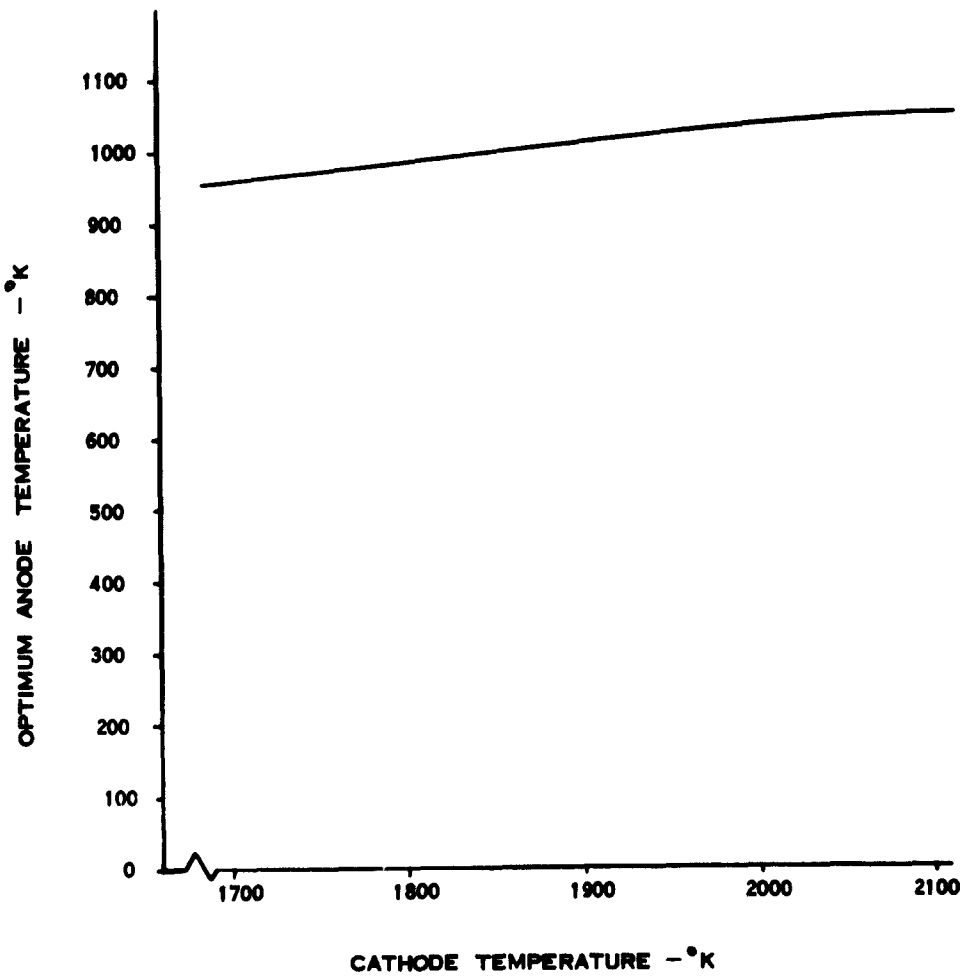

Figure 2. Optimization of Anode Temperature

1.3 Gap Losses

The losses in the converter gap are in the form of:

a) Radiation transferred from cathode to anode

b) Heat conducted through the cesium vapor

c) Electron cooling losses

The radiation loss, q_r, across the gap may be calculated from the relationship:

$$q_r = \frac{\sigma A}{\left(\frac{1}{\epsilon_c} + \frac{1}{\epsilon_a} - 1\right)} \left(T_c^4 - T_a^4\right) \quad (1)$$

where:
- σ = Stephan Boltzman constant = 5.67×10^{-12} w/cm^2 $^oK^4$
- ϵ_c = Emissivity of the cathode = 0.3 @ 1950^oK
- ϵ_a = Emissivity of the anode = 0.15 @ 1030^oK
- T_c = Cathode Temperature - ^oK
- T_a = Anode Temperature - ^oK
- A = Projected cathode anode area = 2.85 cm^2

Solving (1) for q_r, we have:

$$q_r = \frac{(5.67)(2.85)}{(3.33 + 6.66 - 1)} (14.41 - 1.12) = 21.4 \text{ watts} \quad (2)$$

The cesium conduction loss, q_{cs}, may be calculated by the method outlined in Reference 2. This yields a loss of:

$$q_{cs} = 7.8 \text{ watts} \quad (3)$$

The electron cooling loss, q_{ec}, may be calculated from:

$$q_{ec} = I\left(V_c + \frac{2kT_c}{e}\right) \quad (4)$$

where:
- I = emission current - amperes
- V_c = Richardson potential - volts
- $\frac{2kT_c}{e}$ = random energy of the electrons - volts

Figure 3 shows a plot of electron cooling losses versus output voltage for various cathode temperatures. Emission data is based on data published in Reference 4. The computations are based on an average cathode-anode area of 3.0 cm^2.

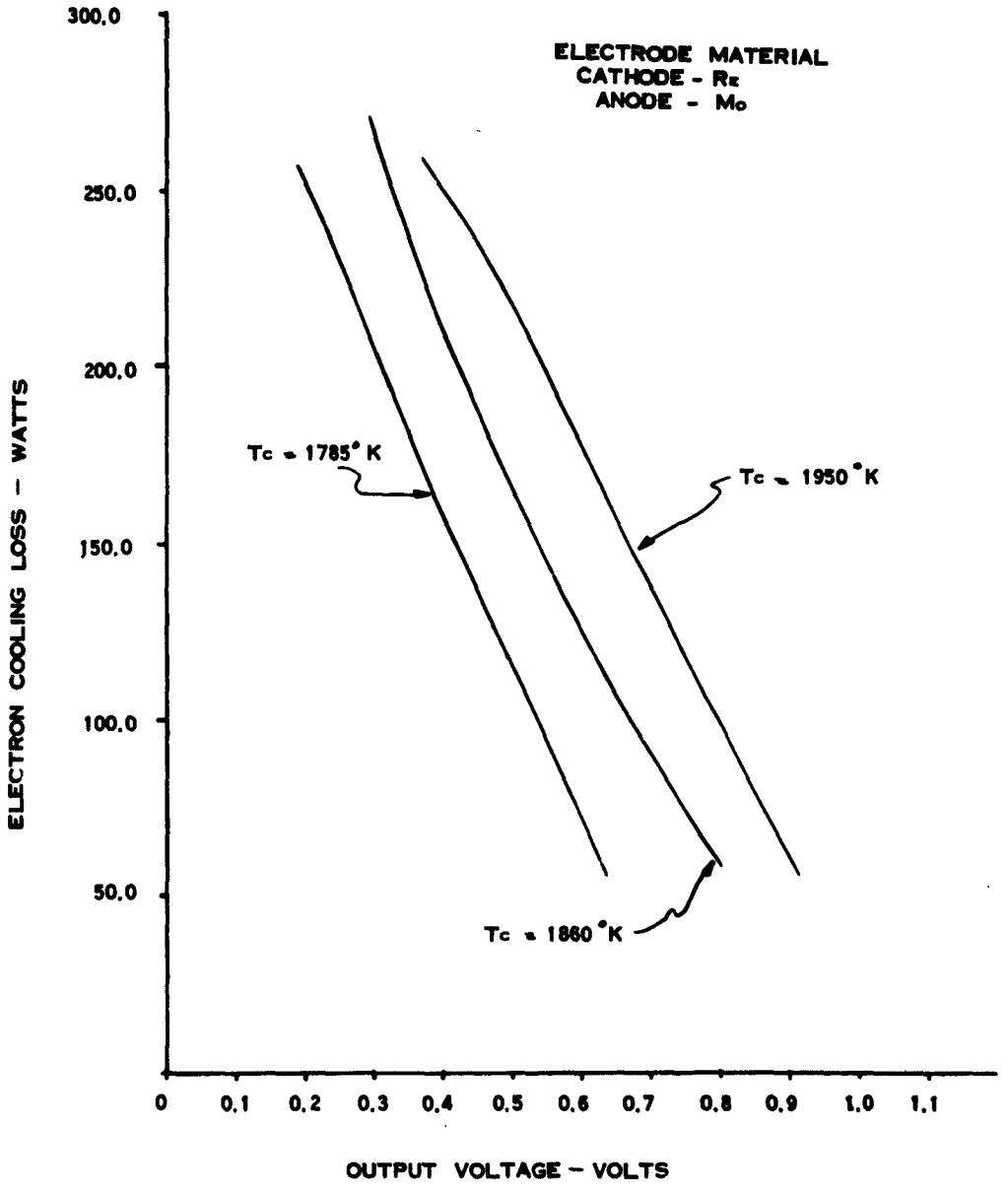

Figure 3. Electron Cooling Loss

1.4 Spacing Method

Spacing of the emitter collector surfaces is accomplished by means of six tungsten pins brazed into alumina caps which are imbedded in the anode surface. This is shown as part #4 in Figure 1. The emitter is held against these pins by a tungsten tensile rod and spring (Figure 1, parts 13 and 18, respectively). The spring is designed to exert a 150 gram force on the collector holding the gap fixed against collector pin structure.

In order to compensate for tendencies of the gap to change due to thermal expansion in the envelope, a flexible bellows configuration has been introduced into the envelope structure. This bellows section also provides a long thermal path to the seal region and effectively shields the seal region from radiation from the higher temperature regions of the envelope and generator.

1.5 Operating Characteristics

In order to determine the losses through the spacing pins and the general operating temperature of the ceramic portion of the spacers, let us assume the following:

a) Radiation from the cathode to the ceramic is negligible compared to the conduction losses since the ceramic area involved is quite small.

b) The temperature of the anode-slug at the point where it makes contact with the ceramic is determined chiefly by other gap losses. The electron cooling loss will account for most of the heat passing through the anode.

Therefore, based on the spacing pin geometry as shown in Figure 1, the following may be defined:

T_c = Cathode temperature
T_{s1} = Temperature of ceramic where pin contacts cup
T_{s2} = Temperature of ceramic at ceramic-anode interface
T_{a1} = Temperature of anode at ceramic-anode interface
q = Heat passing through one spacer pin assembly
k_p = Thermal conductivity of pin = 1.04 w/cm^{o}C
A_p = Cross section area of pin = 0.00425 cm^2
ℓ_p = Length of pin = 0.267 cm
A_c = Cross section area of ceramics base = 0.0324 cm^2
d = Cup bottom thickness = 0.0508 cm
k_c = Thermal conductivity of ceramic = 0.076 w/cm-^{o}K
h = Heat transfer coefficient across contact area between the cup and anode.

Then the following heat balances may be written:

$$q = \frac{k_p A_p}{\ell_p} (T_c - T_{s1}) \qquad \text{conduction through fin} \qquad (5)$$

$$q = \frac{k_c A_c}{d} (T_{s1} - T_{s2}) \qquad \text{conduction through cup base} \qquad (6)$$

$$q = h A_c (T_{s2} - T_{a1})$$ heat transferred across contact between cup and anode-slug (7)

Since the electron cooling loss, radiation loss, and cesium conduction loss will contribute most of the heat transferred to the anode, let us compute the temperature T_{a1} based on this quantity of heat, q_g.

From the previous calculation of gap losses:

$$q_g = q_{ec} + q_r + q_{es} = q_{ec} + 21.4 + 7.8 \quad (8)$$

The peak power point will occur in the vicinity of 0.6 volts at 1950°K. Figure 3 shows an electron cooling loss, q_{ec} = 179 watts at this voltage, which gives:

$$q_g = 179.0 + 21.4 + 7.8 = 208.2 \text{ watts.} \quad (9)$$

Then T_{a1} may be computed, based on the drop across the anode between the anode surface and the shelf surface. A portion of this heat will be transferred by radiation across the slot forming the anode shelf and a portion by conduction through the solid section of the anode slug.

Assuming that the variation of temperature in the radial direction is small in the lower portion of the anode, the drop across the anode slug to the anode side of the shelf slot may be calculated by setting the thermal throughput, q_g, equal to:

$$q_g = \frac{k_a A}{l} (T_a - T_{a2}) \quad (10)$$

$$T_{a2} = 1030 - \frac{(0.125)(208.2)}{(1.11)(0.442)(2.54)} + 1030 = 1030 - 20.8 = 1009.2\ ^{o}K \quad (11)$$

Therefore, assuming uniform temperature radially across the slug:

$$q_g = \frac{\sigma A_s}{\frac{2}{\epsilon} - 1} (T_{a2}^4 - T_{a1}^4) + \frac{k_a A_n}{w} (T_{a2} - T_{a1}) \quad (12)$$

where:
- A_s = Surface area of the slot parallel faces = 1.47 cm^2
- ϵ = Emissivity of slot surfaces ~ 0.3
- σ = Stephan-Boltzman constant = 5.67 x 10^{-12} $w/cm^2\ ^{o}K^4$
- k_a = Thermal conductivity of molybdenum = 1.11 $w/cm\ ^{o}K$
- A_n = Cross section area of anode neck at this point = 1.37 cm^2
- a = Width of the slot = 0.0635

The radiation term becomes negligible for the small temperature difference under consideration and thus:

$$T_{a1} = 1000\ ^{o}K \quad (13)$$

The system of equations given by (5) through (7), must now be solved for T_{s1} and T_{s2}.

The value for the contact resistance may be conservatively estimated from Reference 5 as:

$$h = 0.286 \text{ w/cm}^2 \text{ }^{o}\text{K} \tag{14}$$

for the conditions of pressure and temperature between the ceramic and the anode shelf.

Equating (5) to (6) and (5) to (7) we have:

$$(0.01925)(1950 - T_{s1}) = 0.0664 (T_{s1} - T_{s2}) \tag{15}$$

$$(0.01925)(1950 - T_{s1}) = 0.0916 (T_{s2} - T_{a1}) \tag{16}$$

Solving for T_{s1} and T_{s2}, we have:

$$T_{s1} = 1646 \text{ }^{o}\text{K} \tag{17}$$

$$T_{s2} = 1543 \text{ }^{o}\text{K} \tag{18}$$

The heat lost through each spacer pin is:

$$q = 5.02 \text{ watts/pin} \tag{19}$$

The total spacer loss, q_{sp}, is therefore:

$$q_{sp} = 30.12 \text{ watts} \tag{20}$$

1.6 Anode Fin Sizing

The anode fin operating temperature must be determined by the following criteria:

a) The fin temperature and radiating area must be sufficient to dissipate the heat delivered to the fin.

b) The fin root temperature must be commensurate with safe seal operating temperature.

c) The fin size must be minimized in order to keep overall converter weight down.

In order to insure long seal life, the seal temperature should be maintained at 870°K or less. Since the seal will run at slightly higher temperatures than the fin root, the fin root temperature must be lower still. Reducing the fin temperature necessarily requires an increase in fin area and consequently fin weight. Thus, these two requirements are somewhat in conflict and require some tradeoff.

In order to maximize fin effectiveness, the fin material will be OFHC copper. This allows a thinner and consequently, lighter fin to be used.

The fin and anode slug will be sized at peak power operation at 1950°K. At other operating points, the fin may be partially shielded in order to achieve the proper anode operating temperature.

At 1950°K, a rough calculation shows that the peak power point will occur at approximately 0.63 volts. Thus, from Figure 3, the electron cooling loss is 165 watts. Also, the heat transferred by radiation from the envelope to the anode slug will be approximately 27 watts. Thus, the total heat, q_{Ta}, delivered to the anode fin through the anode slug will be the sum of: the radiation across the gap, the cesium conduction loss, the heat radiated to the anode from the envelope, the heat lost through the spacers, and the electron cooling loss. This gives:

$$q_{Ta} = 251.3 \text{ watts} \tag{21}$$

Since the spacing mechanism fixes the structure of the anode, and the thermal distribution in this area is known, the thermal balance between the anode slug and radiating fin may be written as:

$$q_{Ta} = \frac{k_a A_a}{\ell_a - 0.32} (T_{a1} - T_f) \tag{22}$$

$$q_{Ta} = \eta \sigma \epsilon A_f T_f^4 \tag{23}$$

where:
- k_a = Thermal conductivity of the anode slug = 1.18 w/cm °K
- A_a = Cross section area of the anode = 2.39 cm^2
- ℓ_a = Length of the anode slug from the anode surface to the fin
- η = Fin effectiveness
- σ = Stephan-Boltzman constant = 5.67 x 10^{-12} w/cm^2 $°K^4$
- A_f = Surface area of the anode fin
- T_f = Temperature of the anode fin root - °K
- T_{a1} = Temperature of anode shelf

The copper fin with 65 mil thickness allows a fin effectiveness of 0.86. The fin will be coated with an aluminum-silicon coating which has an emissivity of approximately 0.82 in the temperature range under consideration.

Therefore, solution of Equations (22) and (23), as a function of fin root temperature, for ℓ_a and A_f, gives the curves shown in Figure 4.

Since there may be as much as a 50 °C drop across the seal, the anode fin root temperature will be selected as 820°K. This requires a radiating area of 139 cm^2 and an overall anode slug length of 2.34 cm, as determined from Figure 4.

1.7 Envelope - Lead Optimization

The overall length of the converter has been established by selecting the anode fin temperature and thus, the anode slug geometry. In addition, the bellows configuration of the spacing assembly is fixed. Therefore, the only portion of the lead - envelope

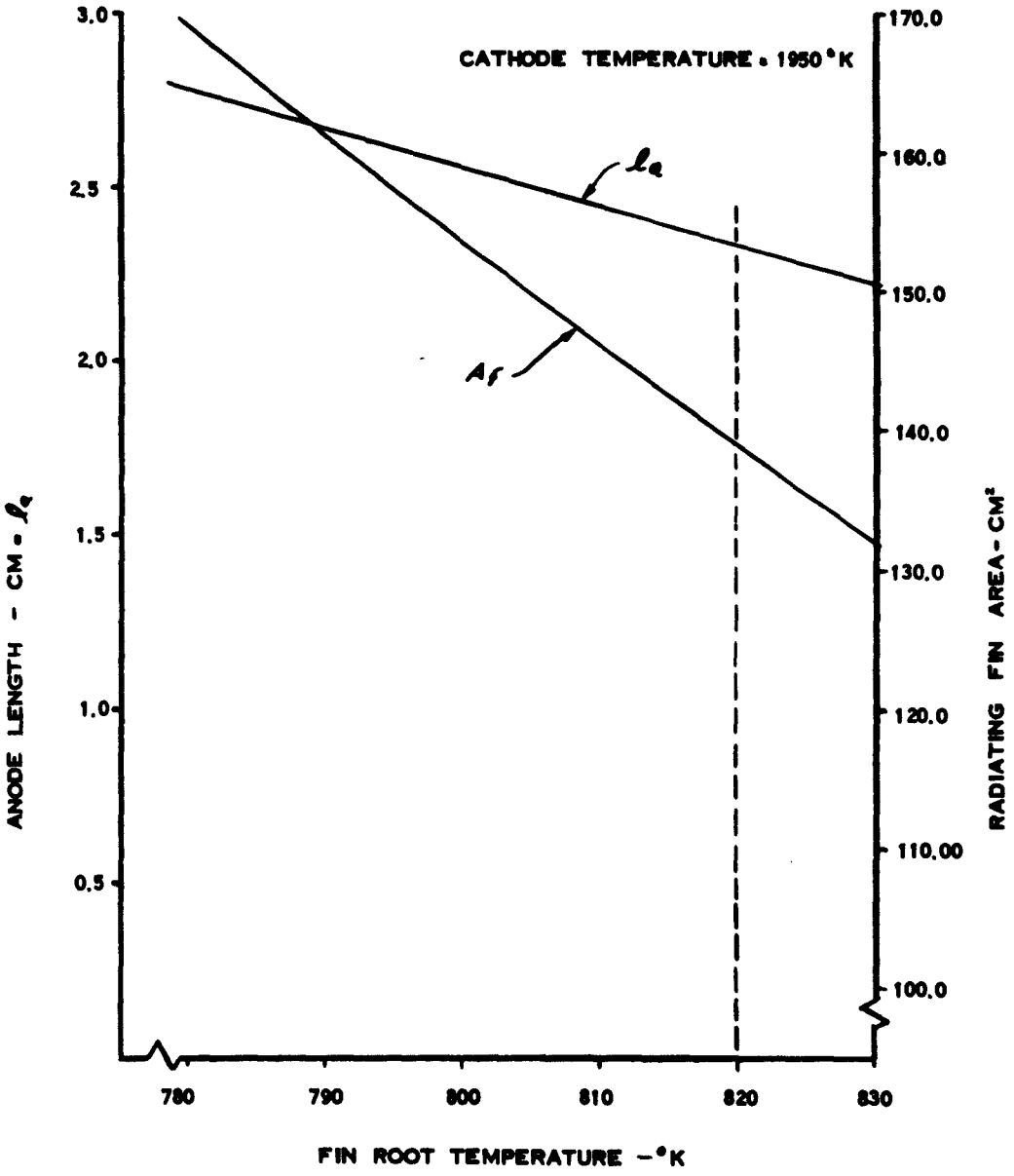

Figure 4. Optimization of Anode Geometry for Peak Power

geometry that can significantly contribute to the electrical resistance losses and thermal conduction losses, is the tantalum envelope section below the bellows.

The efficiency of the device, η, will be expressed as:

$$\eta = \frac{P - P_{\Omega}}{Q_T + Q_{ce}} \tag{24}$$

where: P = Electrical power output available at the cathode-anode before lead losses - watts.

P_{Ω} = Resistive loss in the leads - watts given by I^2R_e

where: I = Output current - amperes

R_e = Electrical resistance of leads - ohms

Q_T = Total thermal throughput including electron cooling losses, gap losses, and envelope radiation to the anode slug - watts

Q_{ce} = Thermal losses by conduction down the envelope and leads - watts.

The heat conducted down the leads, Q_{ce}, may be expressed as:

$$Q_{ce} = \frac{(T_c - T_f)}{R_{TB}} \tag{25}$$

where: R_{TB} = The thermal impedance of the leads - ^{o}K/watt

T_c = Cathode temperature - ^{o}K

T_f = Fin temperature at electrical feed-through - ^{o}K.

Therefore, calculation of efficiency as a function of ℓ/A ratio of the emitter envelope and output voltage results in Figures 5 and 6. On the basis of optimum efficiency, these show the optimum ℓ/A ratio in the vicinity of $\ell/A = 30$, yielding an efficiency of 10.6% with a power output of 23.8 watts at peak efficiency. However, looking at the variation of power output with efficiency we find that while peak efficiency varies from 10.4% to 10.6%, the respective peak power output varies from 30.9 watts to 26.9 watts. Therefore, for an increase of only 0.2% in efficiency we take a decrease of 4.0 watts in usable power output. Since the 0.2% in efficiency is well within calculation error, it is more reasonable to accept a slightly less efficient converter with a thicker envelope.

1.8 Predicted Converter Performance at 1950^{o}K

Figure 7 indicates the predicted efficiency and power output of the converter at 1950^{o}K cathode temperature, based on the emission data used and the preceding calculations.

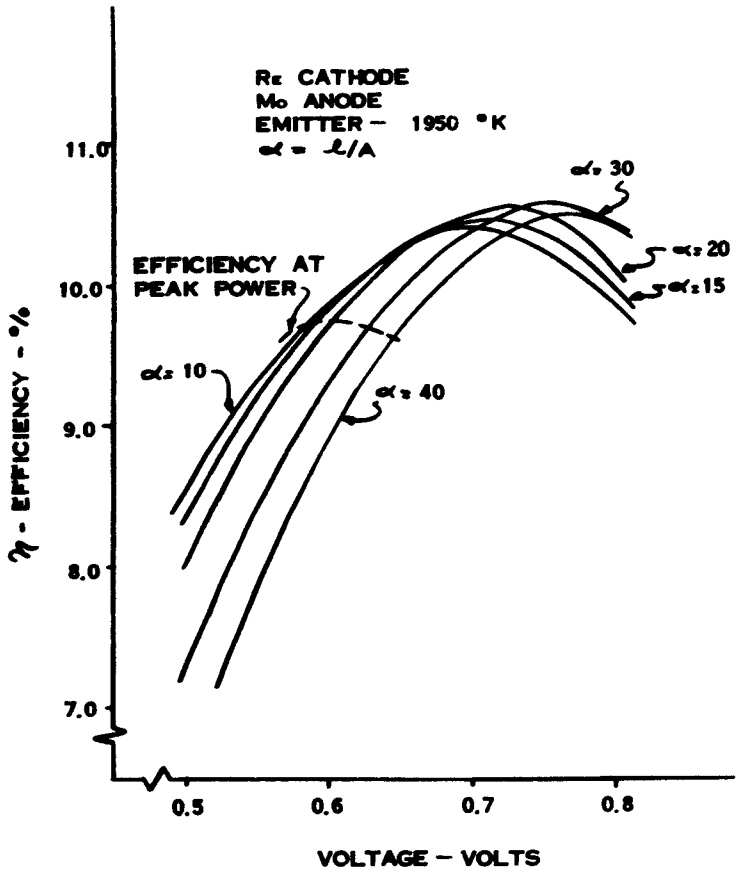

Figure 5. Converter Efficiency with Optimized Lead Geometry

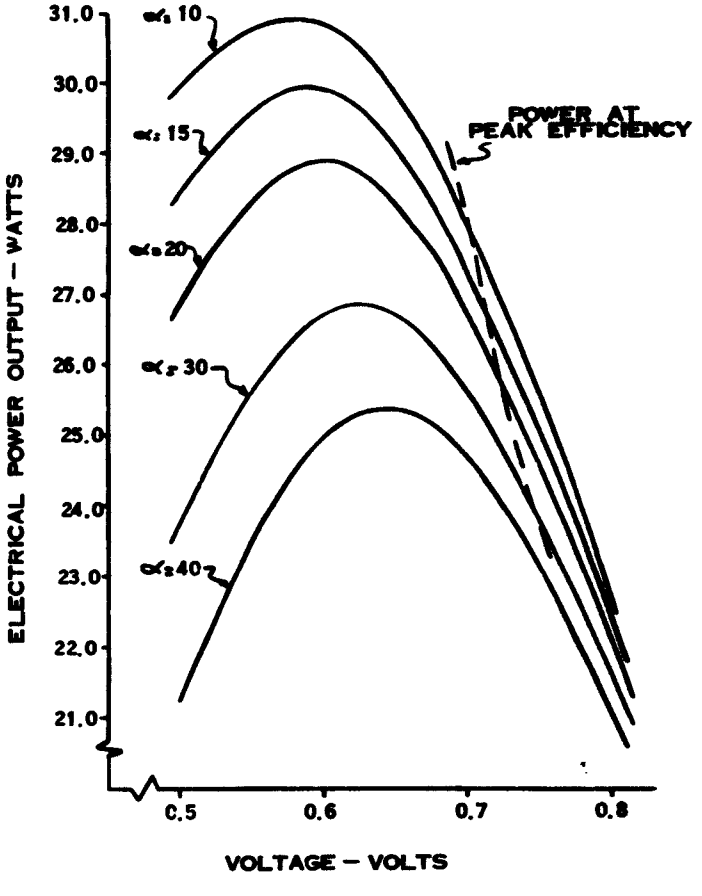

Figure 6. Converter Power Output with Optimized Lead Geometry

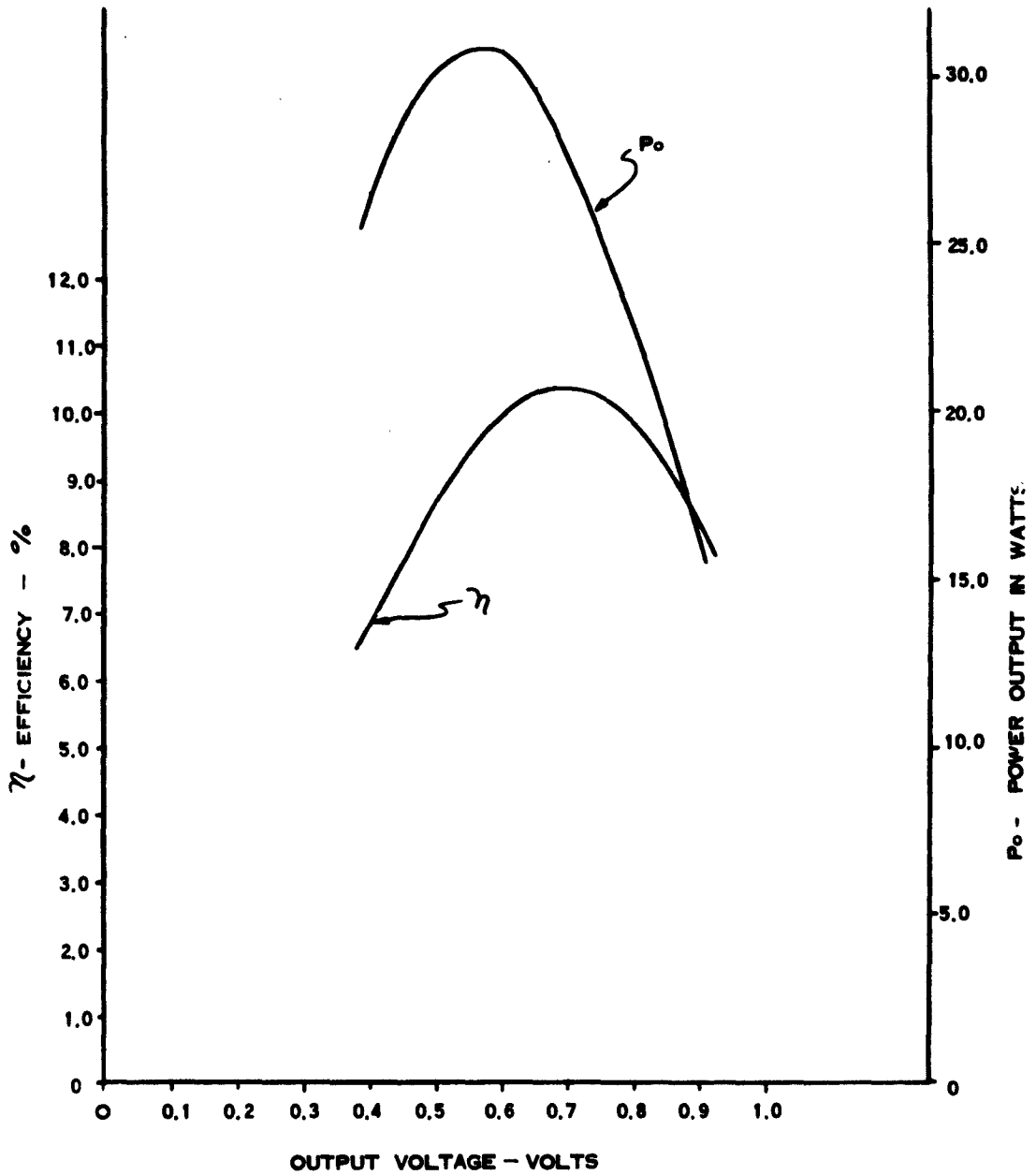

Figure 7. Predicted Converter Power and Efficiency

2.0 GENERATOR DESIGN AND ANALYSIS

2.1 Generator Design

The "integral generator," selected as the best design to meet the objectives of the STEPS III program, is shown in Figures 8 and 9. These figures, respectively, show configurations for solar and laboratory (electron bombardment) test evaluation. The generator sections that contain the converters are identical for solar and laboratory configurations but the front and back generator sections differ.

This generator was designed to serve dual purposes as follows:

a) Complete generator unit for solar or laboratory evaluation, to advance the state-of-the-art toward obtaining larger power output at usable voltage levels with low specific weight.

b) Calorimeter to determine single or multiple converter performance by accurate measurement of converter efficiency in either solar or laboratory testing.

Generator design and analysis is based on a four-converter configuration,with all converters in one plane suitable for operation in the 1750-1950^{o}K temperature range. Converters with a cathode area of 3 cm^{2} are used giving a total emitting area of 12 cm^{2} for the generator. Various design concepts and specific insulations have been evaluated (see Reference 1) with respect to thermal efficiency, weight, life, fabricability, and mechanical integrity. The design is an extension of the CVG three-converter design reported in Reference 2 and evaluated in solar testing for over 130 hours above its design point temperature of 1650^{o}K.

Significant features of the integral generator design are:

1) Anode fins form generator frame, simplifying the design, reducing weight, and providing the converter alignment reference.

2) Reduced complexity of the generator, allowing simpler configuration of parts (such as, cathode shoes or radiation shields), wider tolerances, and lower fabrication costs.

3) Improved insulation efficiency through the use of more shields in less space than the CVG design. (Use of .002 inch shields allow 134 shields per inch of thickness.)

4) Reduced weight primarily through the use of molybdenum radiation shielding and using anode fins as the generator frame.

5) Heat losses through joints between radiation shields is minimized through the use of tungsten wool fillers, right angle shields (see Reference 1), and wider tolerances.

6) Generator insulation life should be greater than 10,000 hours with the use of twelve tantalum shields at the high temperature cavity boundary to avoid the vapor pressure problem. Molybdenum can be used satisfactorily for all remaining shields.

7) Cavity similarity with CVG is retained so test results can be easily compared.

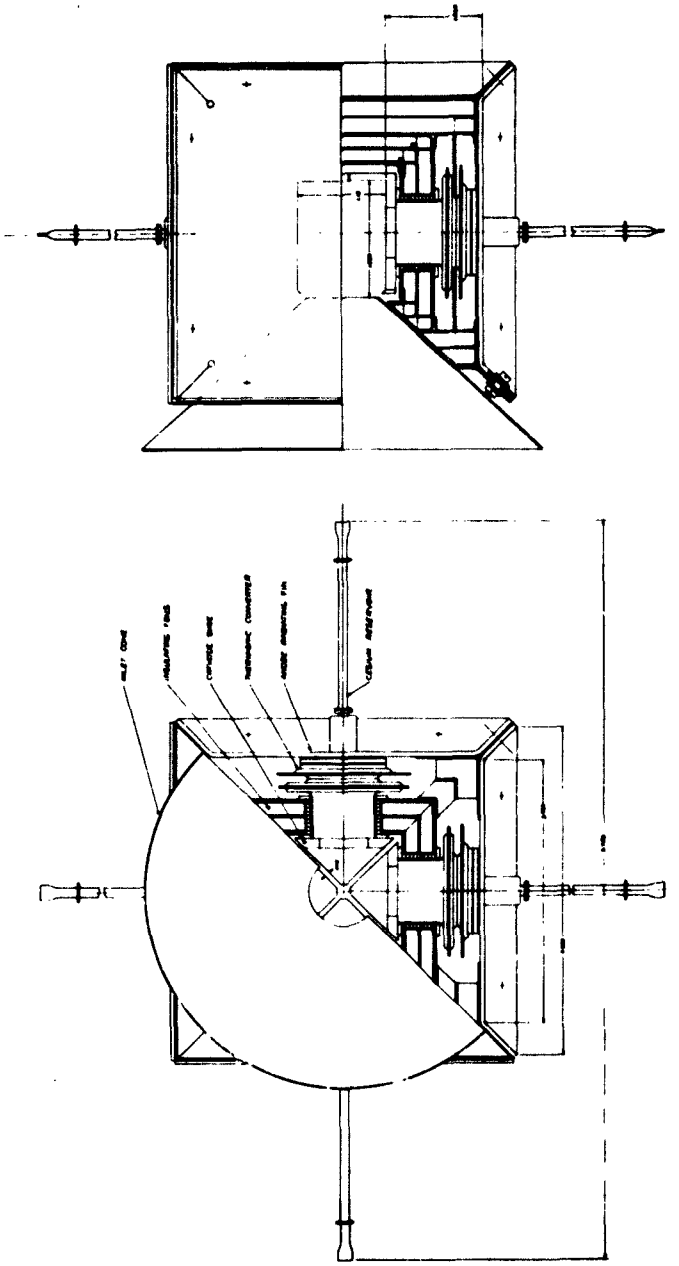

Figure 8. Generator Layout - Solar Test

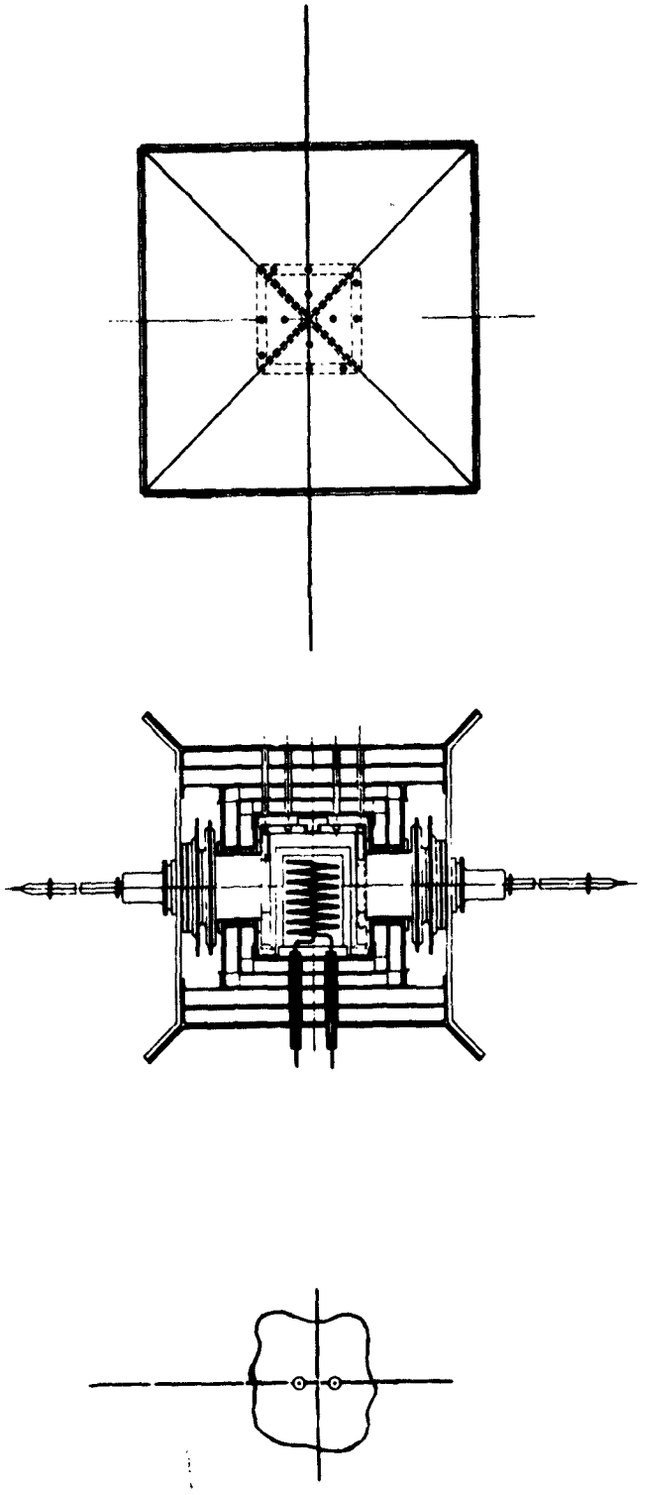

Figure 9. Generator Layout - Laboratory Test

Since the generator is fabricated in individual sections, it can serve the purpose of a high temperature calorimeter to evaluate converter efficiency. This is done by fabricating sections without the opening for the converter, and measuring thermal loss from a generator or calorimeter made up of four blank converter sections plus the front and back sections. Then, by introducing a single converter, its efficiency can be accurately determined. Accurate values of efficiency are particularly important since the weight of a total solar thermionic power system is primarily dependent on converter and generator efficiency. The present design could be used to accurately measure efficiency in either solar or laboratory testing.

2.2 Generator Analysis

2.2.1 Performance Expected

Performance of the STEPS III generator has been predicted for both solar and laboratory testing for the design-point temperature range of 1750-1950°K. This analysis is based on the collector generator system study of Reference 1, on the analyses of thermal loss subsequently outlined in this report, and on the expected converter performance as summarized in Figure 7.

Based on these results, a total power of 1790 watts is required for the generator, with four 3 cm^2 converters, in a ground based solar test in the General Electric Solar Test Facility in Phoenix, Arizona. At 1950°K with converters operating at peak power, an overall generator efficiency of 6.5% is expected. This represents electrical power output divided by all solar power entering the cavity. For the same condition, but with converters at predicted peak efficiency, the generator power requirement is 1585 watts and the generator efficiency is 6.8%. As a comparison, the CVG generator, described in Reference 2, has attained 2.8% generator efficiency when operating at 1940°K, although it was designed to operate at 1650°K.

An estimate of generator performance in a space environment and with solar insolance of 130 watts/ft^2 has also been made. A collector reflectivity of 0.90 and a shadow area of 5% were assumed. Calculations were made for three collector diameters, 5, 3.5 and 2 ft, with 45° rim angle. Orientation accuracy of six minutes was assumed. The power entering the aperture under these conditions is shown in Figure 10. Subtracting cavity reflection, re-radiation, and aperture-cone losses, the net energy available to the generator for thermal loss and converter power is shown in Figure 11. The maximum values for net available power cross-plotted versus cathode temperature are shown in Figure 12.

Based on the subsequent analysis of generator losses and expected converter performance, the generator is expected to require 1320 watts net power at 1950°K cathode temperature. Interpolating from Figures 11 and 12, this power could be supplied by a collector of 4.2 ft diameter and an aperture of 0.77 inches. For these conditions, the overall generator efficiency at converter peak power will be 7.2%, and the overall system efficiency will be 6.4% in space.

Performance of the generator in the laboratory, with an electron bombardment heater as shown in Figure 9, has also been estimated. For the laboratory configuration with four (4) converters operating at 1950°K at peak power, the expected efficiency is 9.4%. The higher efficiency for laboratory testing is due to the lack of aperture losses.

Generator power requirements for operation at 1750°K, 1850°K, 1950°K temperatures, used to predict generator performance, are calculated by methods to be outlined later in this report. Results of the calculations are given in Table 1, with the tabulated values of converter thermal requirements being based on Figure 13. The thermal losses, as shown in Table I, give a means of relatively comparing the contribution of each com-

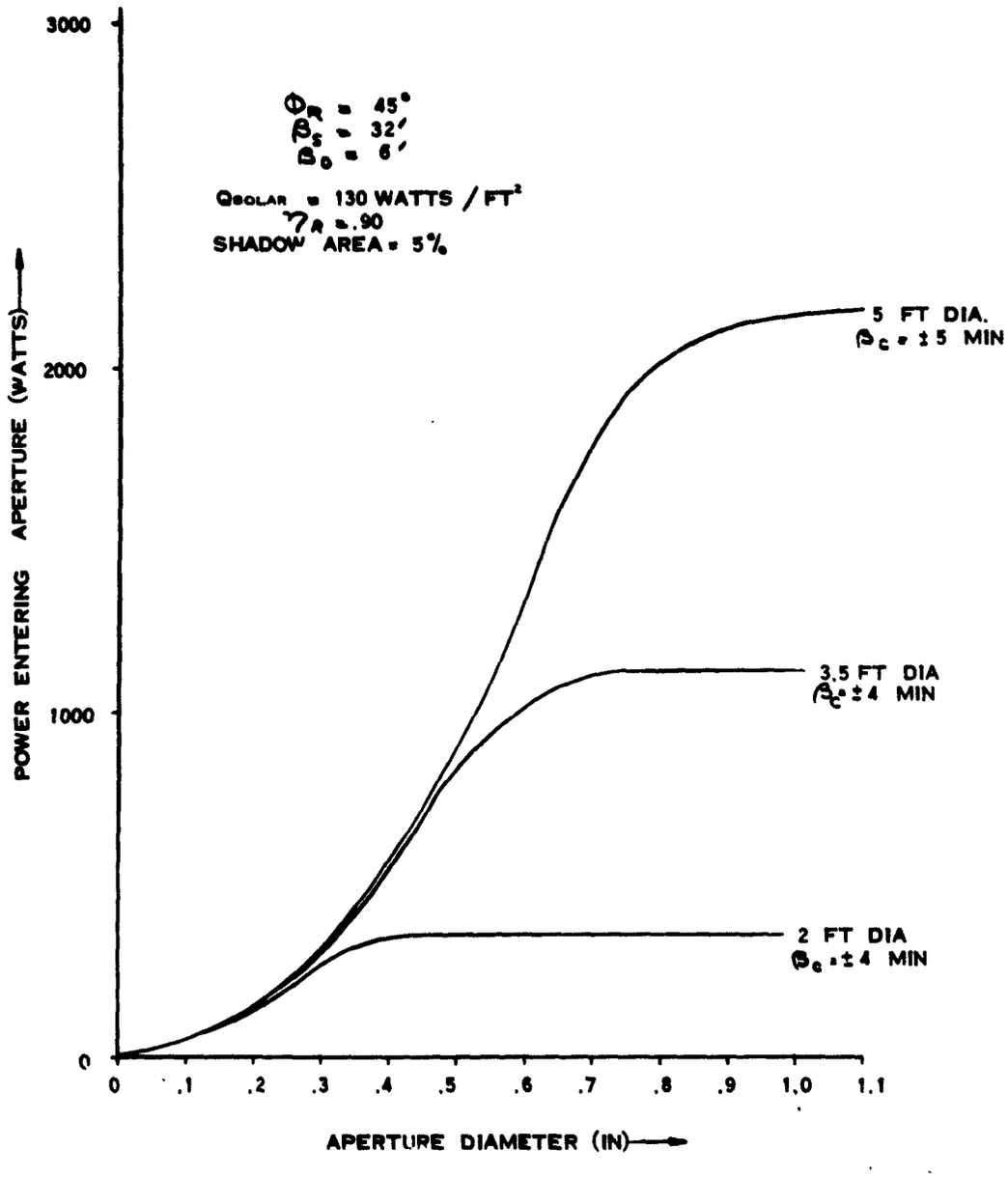

Figure 10. Power Entering Aperture in Space

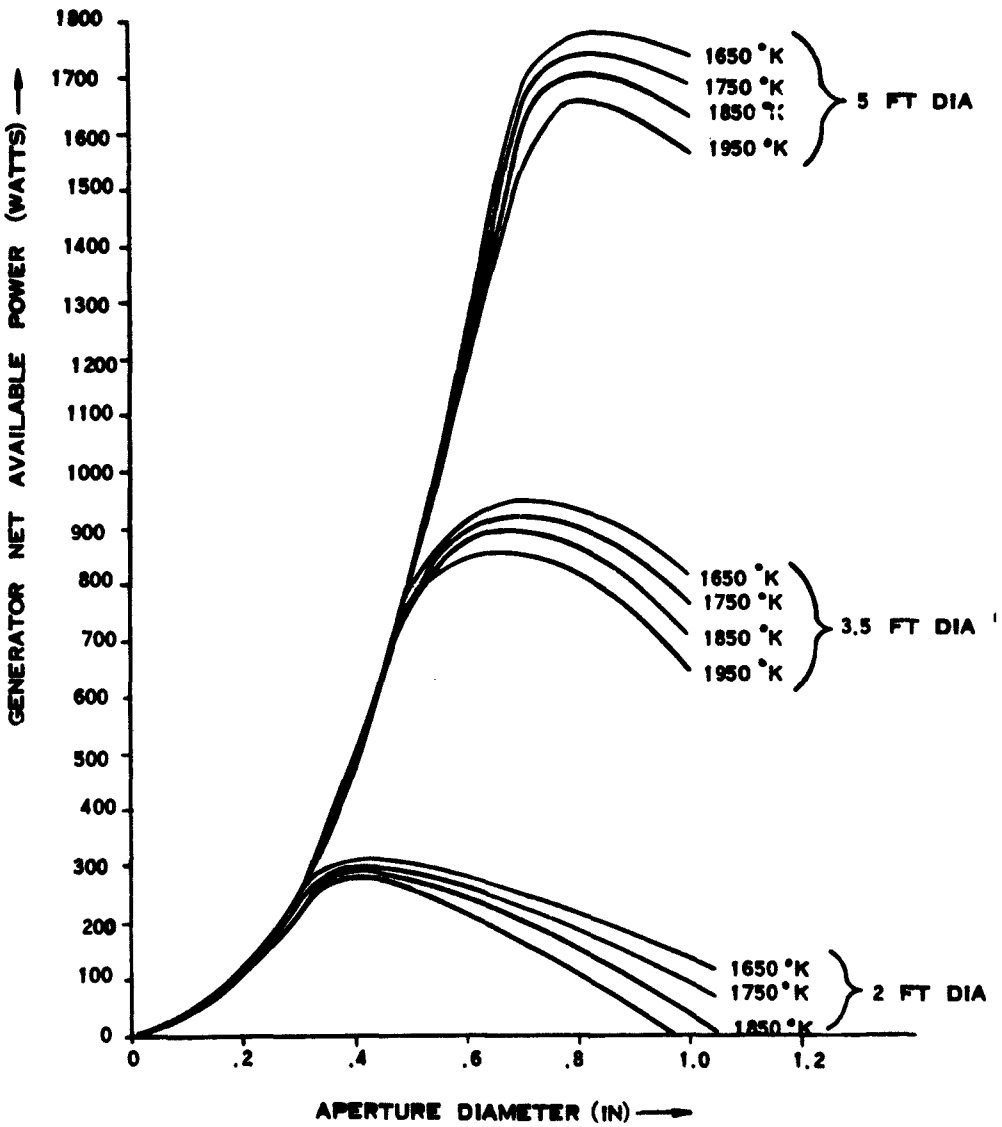

Figure 11. Generator Net Available Power in Space

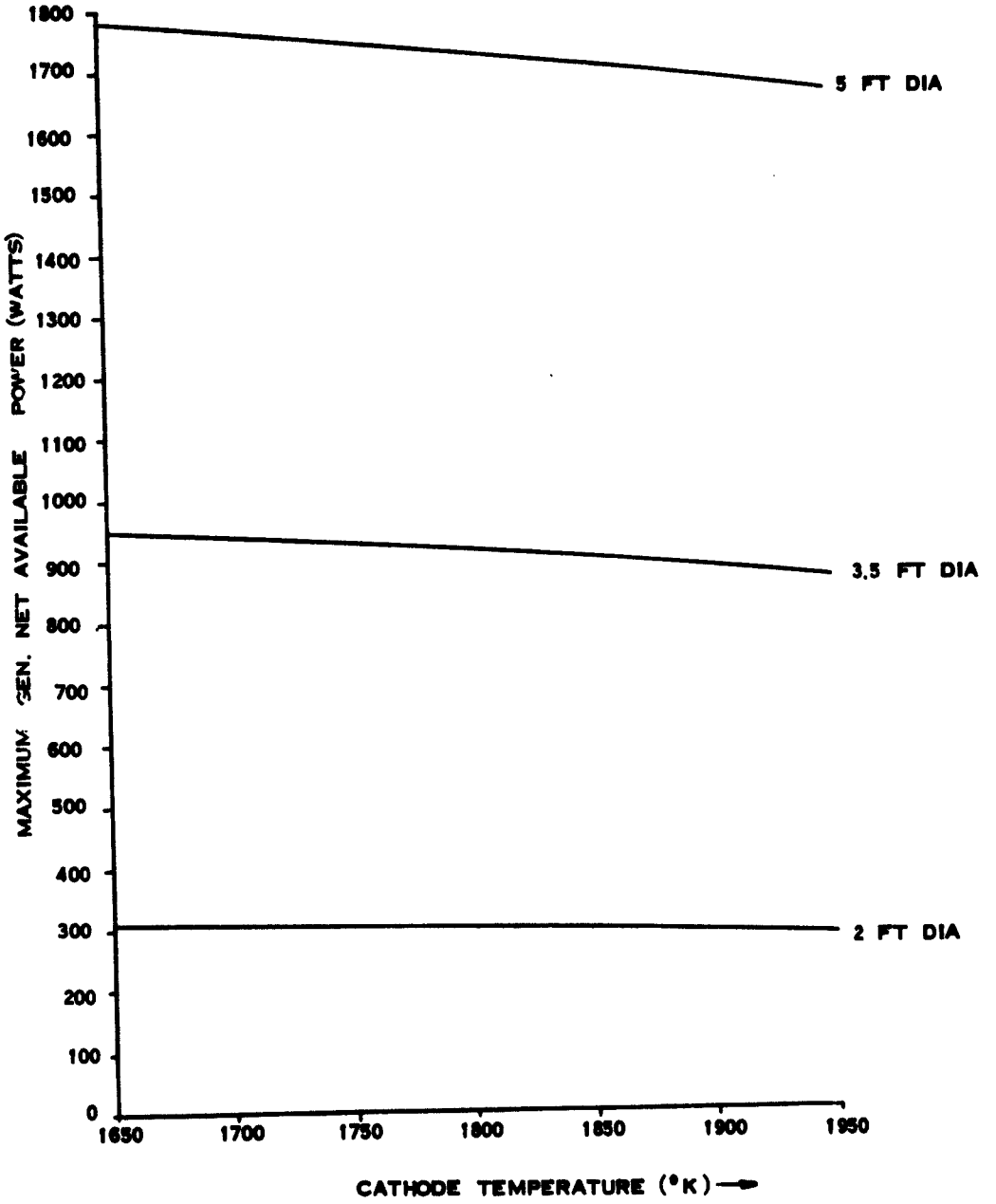

Figure 12. Maximum Generator Net Available Power in Space

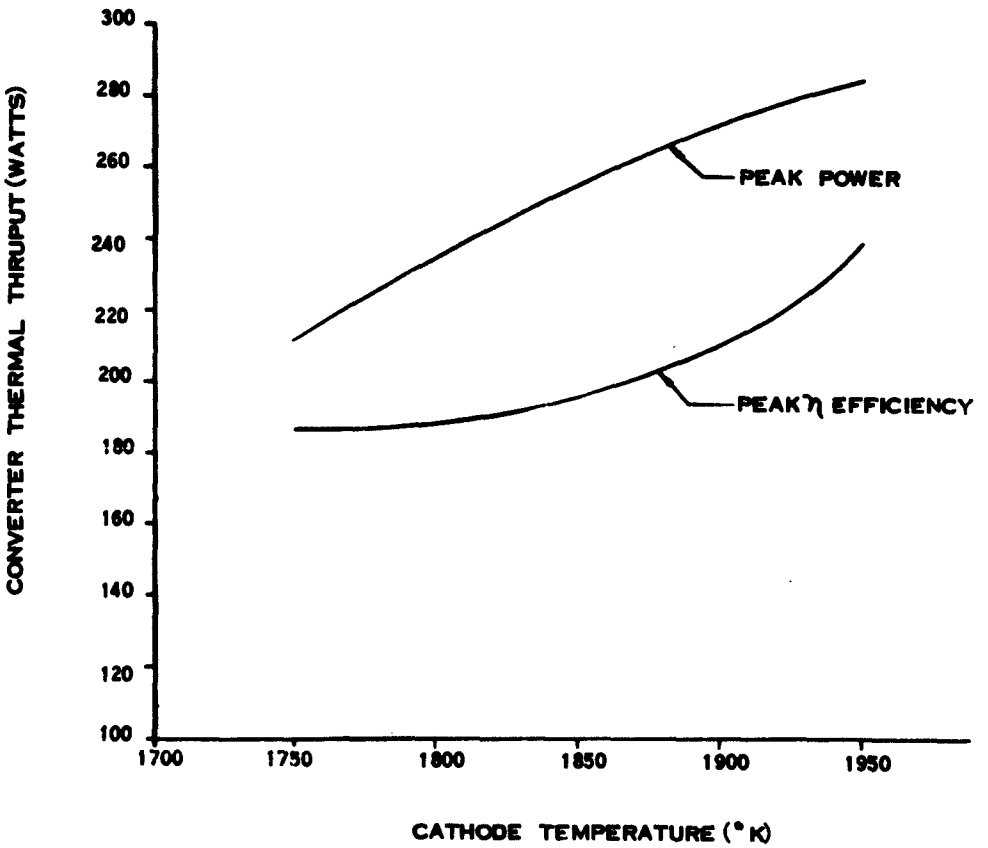

Figure 13. Converter Thermal Throughput

TABLE 1. STEPS III GENERATOR, PREDICTED THERMAL POWER REQUIREMENTS

(Power requirements and thermal losses are tabulated in watts)

		CATHODE TEMPERATURE		
		1750°K	1850°K	1950°K
Components - Solar Test:				
Converter (1)	Peak Power	212	256	284 watts
	Peak Efficiency	187	196	238
Cavity Reradiation & Reflection		192	241	300
Aperture Cone		86	91	94
Converter Section (1)				
	Radiation Shields	7.8	9.8	12.2
	Support Wires*	1.1	1.2	1.3
Front Aperture Section (1)				
	Radiation Shields	4.3	5.3	6.6
	Support Wires*	0.2	0.2	0.2
Back Section (1)				
	Radiation Shields	7.4	9.2	11.5
	Support Wires*	0.2	0.2	0.2
Additional Laboratory Test and Calorimeter Components:				
Dummy Converter Section (1)				
	Radiation Shields	8.0	10.0	12.4
	Support Wires	0.4	0.4	0.4
Front Heater Section (1)				
	Radiation Shields	7.4	9.2	11.5
	Support Wires	0.2	0.2	0.2
Heater Lead Ceramics (2)		4.5	4.7	5.0
Thermocouple Leads & BeO Insulator (1)		2.5	2.6	2.8

*Wires that support and hold radiation shields in position.

ponent to the total thermal loss. The relatively small values of thermal loss through the radiation shielding are indicative of the accuracy with which this generator can serve as a calorimeter to measure absolute converter efficiency.

2.2.2 Thermal Losses Through the Insulation

The insulation used in this generator is composed of multiple radiation shields, of .002" thick molybdenum, held apart by .006" high dimples. The shields are supported by .010" tungsten-rhenium wires.

Radiant heat loss through a multiple radiation shield assembly, with shields of equal emissivity, is given by:

$$\frac{Q}{A} = \frac{\sigma (T_a^4 - T_B^4)}{\frac{1}{\epsilon_A} + \frac{1}{\epsilon_B} - 1 + N\left(\frac{2}{\epsilon_N} - 1\right)} \tag{26}$$

and

$$Q/A = \sigma (T_B^4 - T_o^4) \epsilon_B \tag{27}$$

where: Q/A = Radiant heat transfer per unit area

σ = Stefan-Boltzman constant

T = Temperature

ϵ = Emissivity of the shields

N = Number of shields

and: subscripts A and B refer to the inside (cavity) and outside shields of the assembly respectively. Subscript 0 refers to the external environment.

Combining Equations (26) and (27) to eliminate T_B, gives:

$$T_B^4 = \frac{T_o^4 + \frac{T_A^4}{\lambda}}{1 + \frac{1}{\lambda}} \tag{28}$$

where:

$$\lambda = \epsilon_B \left[\frac{1}{\epsilon_A} + \frac{1}{\epsilon_B} - 1 + N\left(\frac{2}{\epsilon_N} - 1\right)\right] \tag{29}$$

introducing (29) into (26):

$$Q/A = \frac{\sigma \epsilon_B}{\lambda} \left[T_A^4 - \left(\frac{T_o - T_A^4/\lambda}{1 + \frac{1}{\lambda}}\right)\right] \tag{30}$$

Heat loss through the wires that support the radiation shields is given by:

$$Q = K A \frac{\Delta T}{L} \tag{31}$$

where: K = Conductivity

A = Wire cross-sectional area

L = Wire length

ΔT = Temperature differential between the ends of the wire.

The heat loss through the various sections of the generator has been calculated from these equations and is given in Table 1. The external environmental temperature for both laboratory and ground-solar testing is assumed to be 300°K. Effective emissivity of the molybdenum and tantalum radiation shields has been assumed as 0.3. The emissivity of the anode fins, which form the outer frame of the shield package is assumed as 0.8. Experimental evaluation of the CVG shielding indicated that use of these values, with conduction through dimples neglected, gave close correlation with total heat transfer through the shielding.

2.2.3 Re-Radiation and Reflection Losses

The cavity solar absorptivity for the STEPS III generator, (Reference 6) is given by:

$$F_A = \frac{\alpha}{1 - (1 - \alpha)(1 - \theta)} \tag{32}$$

where: F_A = Cavity solar absorptivity

α = Cathode shoe solar absorptivity

θ is defined as the average fraction of light which is either reflected or emitted from the surface of cavity interior, and passes directly out of the aperture. This view factor θ is highly complex and difficult to obtain for the variety of cavities which may be used.

The cavity reradiation loss is given by:

$$Q_R = F_R \sigma T_c^4 A_c \tag{33}$$

where: T_c = Cavity temperature (°K)

A_c = Cavity inside surface area (in^2)

σ = Stephan-Boltzman constant

= 3.657×10^{-11} watts/in^2 $°K^4$

F_r is defined by:

$$F_R = \frac{\epsilon \theta}{1 - (1 - \theta)(1 - \epsilon)} \tag{34}$$

where: ϵ = Total hemispherical emissivity of cathode shoe material

For a cylindrical shaped cavity a numerical procedure has been developed based upon the configuration factors described in Reference 7. The cylinder of radius R_c and length L is divided into a number of small rings of length Δ L and area A_i. The configuration factor, F_i, of one of these rings with respect to the cavity aperture radius, R_A, is given by:

$$F_i = \frac{X}{R_c}\left[\frac{1+\frac{R_A^2}{R_c^2}+\frac{X^2}{R_c^2}}{\sqrt{\left(1+\frac{R_A^2}{R_c^2}+\frac{X^2}{R_c^2}\right)^2-4\frac{R_A^2}{R_c^2}}}-1\right] \tag{35}$$

where: X = Distance from the aperture.

This function has been tabulated and is illustrated in Figure 14.

In addition, the configuration factor for the rear or back disc of the cavity can be calculated from:

$$F_{i_R} = 1/2\left(X - \sqrt{X^2 - 4E^2D^2}\right) \tag{36}$$

where: $E = \frac{R_A}{L}$

$X = 1 + (1 + E^2)D^2$

$D = \frac{L}{R_c}$

This function has been tabulated and shown on Page 104 of Reference 8.

Since configuration factor has been defined as the portion of energy leaving the area under consideration which passes out the aperture, θ can be given as:

$$\theta = \frac{\sum_{i}^{L} A_i F_i + A_R F_{iR}}{A_c} \tag{37}$$

where: A_c = Cavity internal surface area

F_i = Configuration factor for cavity side ring

A_i = Area of cavity side ring

A_R = Area of cavity rear

F_{i_R} = Configuration factor for cavity rear

The summation in Equation (37) indicates that the areas and configuration factors of the cavity are summed over the cavity length.

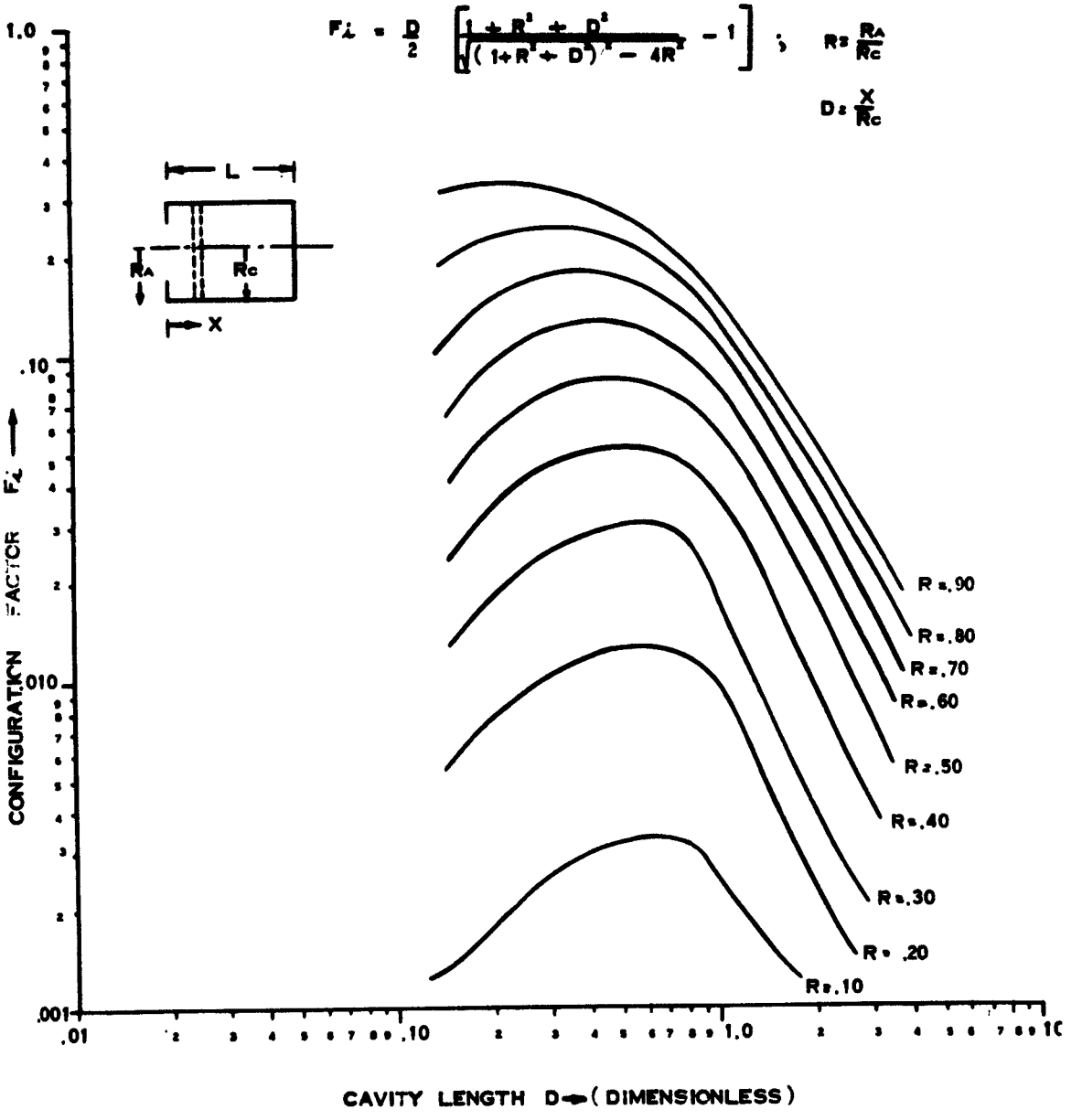

Figure 14. Configuration Factor for Cavity Sides

The STEPS III generator cavity is rectangular and is 1.53 inches long and 1.15 inches between cathode surfaces. The inside surface area of the cavity is:

$$A_c = 9.69 - .785\, D_A^2 \quad in^2 \tag{38}$$

where: D_A is aperture diameter.

Although the cavity is rectangular, it will be approximated by a cylinder 1.53 inches long with an equivalent radius R_c of:

$$2\ R_c\,(1.53) + 2\ R_c^2 = 9.69 \tag{39}$$

or

$$R_c = .692 \text{ in.}$$

The cathode shoe material which forms the cavity is tantalum. From Reference 8, the absorptivity and emissivity for tantalum are:

$$\alpha_{TA} = .42$$

$$\epsilon_{TA} = .30$$

Using equations 32, 34 and 37, the cavity solar absorptance and re-radiated power can be calculated versus aperture diameter. These results are shown in Figures 15 and 16. The total loss by reflection and re-radiation at various cathode temperatures has been given in Table 1.

2.2.4 Thermal Loss from Aperture Cone

For the solar test version of the STEPS III generator, one means of heat loss from the cavity is through the aperture cone. Heat that is picked up by the lip of the aperture cone is carried away by conduction along and radiation from the cone. An analysis of this loss is made by considering the cone as a radiating fin. It is assumed that one side of the cone is insulated and that the radiation will be the same as that from a flat circular plate having an area equal to the projected area of the cone.

The cone has an outer diameter of 2.60 inches and is fabricated from .020 inch thick molybdenum. The projected surface area is .0454 sq. ft. Conductivity for molybdenum is 80.6 Btu/hr ft ^{o}F. Emissivity for the highly polished cone is assumed as 0.28. The lip temperature is assumed to be the cathode temperature. The environment temperature is assumed to be 300^{o}K. Values of heat loss for various cathode temperatures are shown in Table 1.

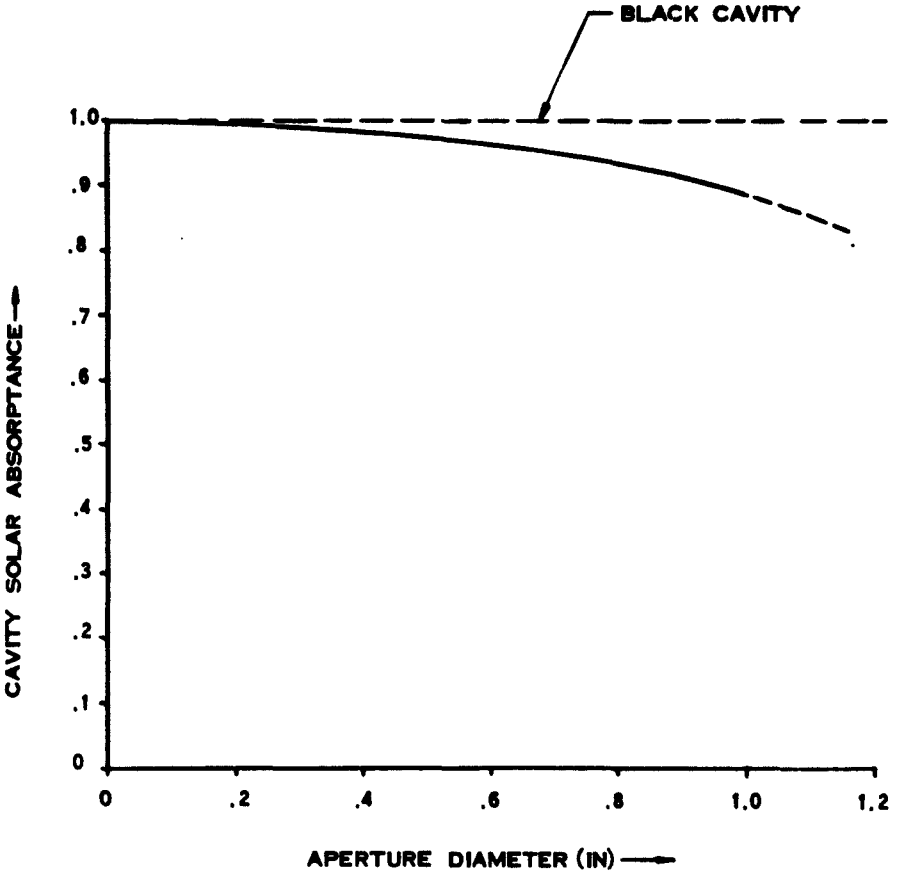

Figure 15. Cavity Solar Absorptance

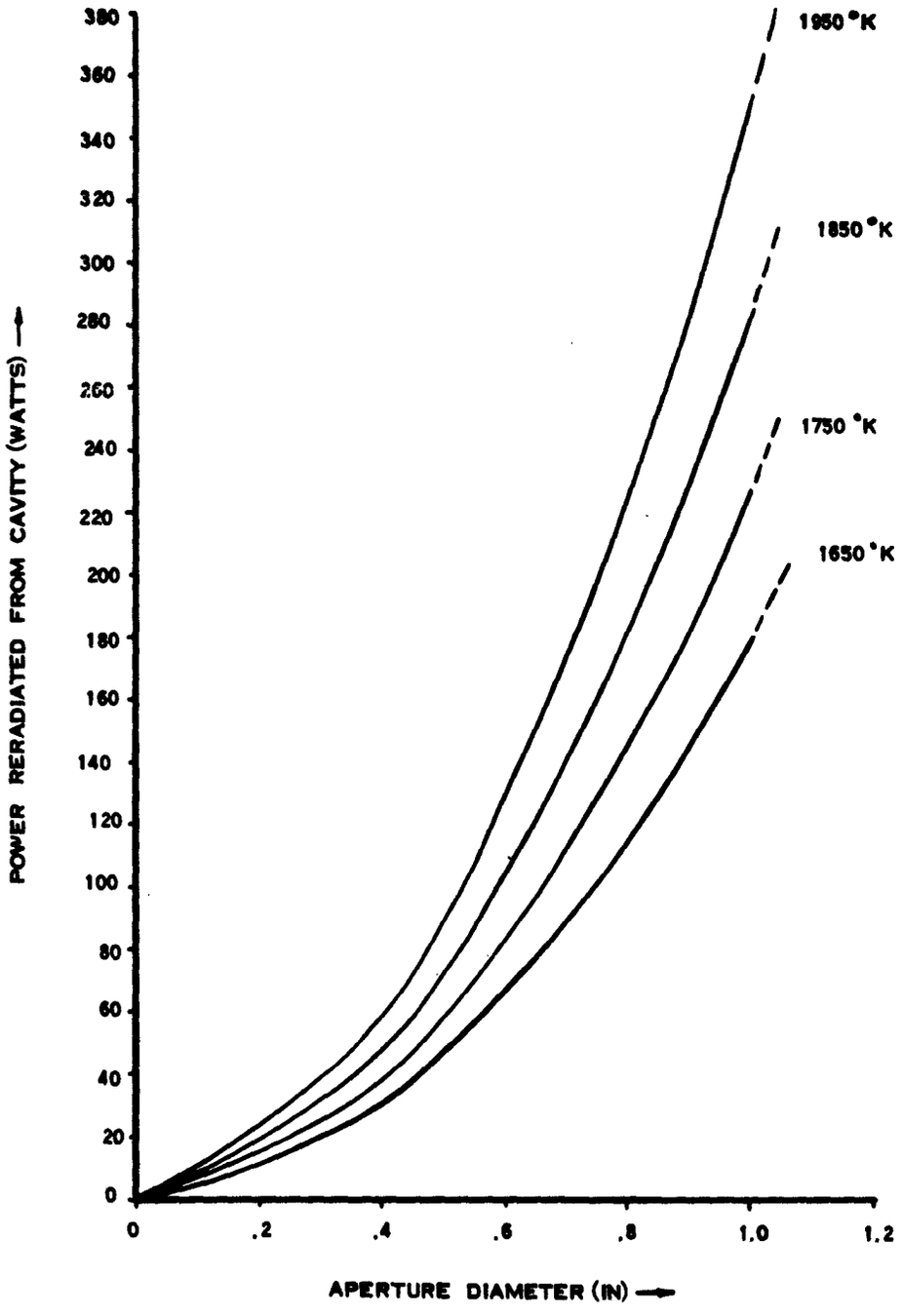

Figure 16. Cavity Reradiation Loss

3.0 CONVERTER TEST RESULTS

3.1 Description of Converters

Three converters of the preliminary A and B Series designs were tested. Although these converters will fit into existing generators, they were primarily built to evaluate certain materials, design concepts, and fabrication techniques and were not optimized for geometry, as were the subsequent C Series converters. However, the test results are significant for obtaining a preliminary estimate of achievable performance on planar converters suitable for use in a solar generator system.

All converters on this program have been designed to hold a relatively constant spacing, both hot and cold, to improve reproducibility. The best method available was the use of pins or posts between the cathode and anode. These pins rest on alumina insulators recessed into the cooler anode, out of the plasma region. Thus, deterioration of the ceramic insulator should not occur as it would if used directly on the hot cathode. Spacing was maintained by designing for a slight pressure on these pins, either through a spring or thermal expansion. Using this technique, measured spacing during cycling varied only 0.0002" between the hot and cold conditions. The inevitable thermal mismatches between anode and envelope expansion rates were accounted for by flexible bellows sections located in the envelope near the metal-ceramic seal.

Description of the converters tested is as follows:

A-1: Mo-Mo at 0.002" spacing
Spacing held constant by 4 - 0.030" W-Re pins resting on the cathode and seated in alumina cups that are recessed into the anode. Pressure on pins is maintained through differential thermal expansion of the anode and envelope. Flexible bellows in envelope adjacent to the seal allow for thermal expansion mismatches.

Cathode Area 3.08 cm^2

Cathode Area minus Pin Area 3.06 cm^2

Anode Area 2.77 cm^2

Anode Area minus Spacing Pin Holes 2.62 cm^2

B-1: Ta-Ni at 0.005" spacing
Spacing held constant by six tungsten pins welded into cathode and resting on an alumina ring around the anode. Pressure on the pins is maintained by a spring loaded tungsten tension rod welded into the cathode and extending through the anode. Flexible bellows in envelope below seal allow for thermal expansion mismatches.

B-2: Mo-Ni at 0.005" spacing
Spacing held constant by six tungsten pins resting on the cathode and seated in alumina cups in the anode. Tension rod and bellows same as B-1.

B-1 and B-2:

Cathode Area 3.28 cm^2

Cathode Area minus Pin Area 3.24 cm^2

Anode Area 2.85 cm^2

Anode Area minus Spacing Pin Holes 2.62 cm^2

3.2 Converter Performance

Converters B-1 and B-2 were both operated more than 50 hours during performance evaluation. Tests were conducted with the converters mounted horizontally in a CVG insulation section, and heated by electron bombardment, as shown in Figure 17. Steady state E-I characteristics of the converters are given in Figure 18 and 19. Two E-I curves are shown at 1950°K for each converter, indicating the best power output obtained and the power output after 40 to 50 hours of operation. In addition, a set of data was generated on the characteristics of the Mo-Ni converter, B-2, showing variation with cesium reservoir and anode fin temperature. This data is given in Figures 20 through 27.

Converter A-1 was tested in the vertical position but power output could not be optimized since the anode was operating too hot. An output of 4.3 watts/cm^2 at 1950°K was achieved. This pin spacing design was heat cycled to 1750°K, with spacing, as measured by capacitance, varying from 0.0018" cold to 0.0020" hot.

Spacing techniques used in both the A and B series designs seemed to work quite well in maintaining constant spacing. Also, no anode-to-cathode shorting problems have been encountered during steady state or cycling operation.

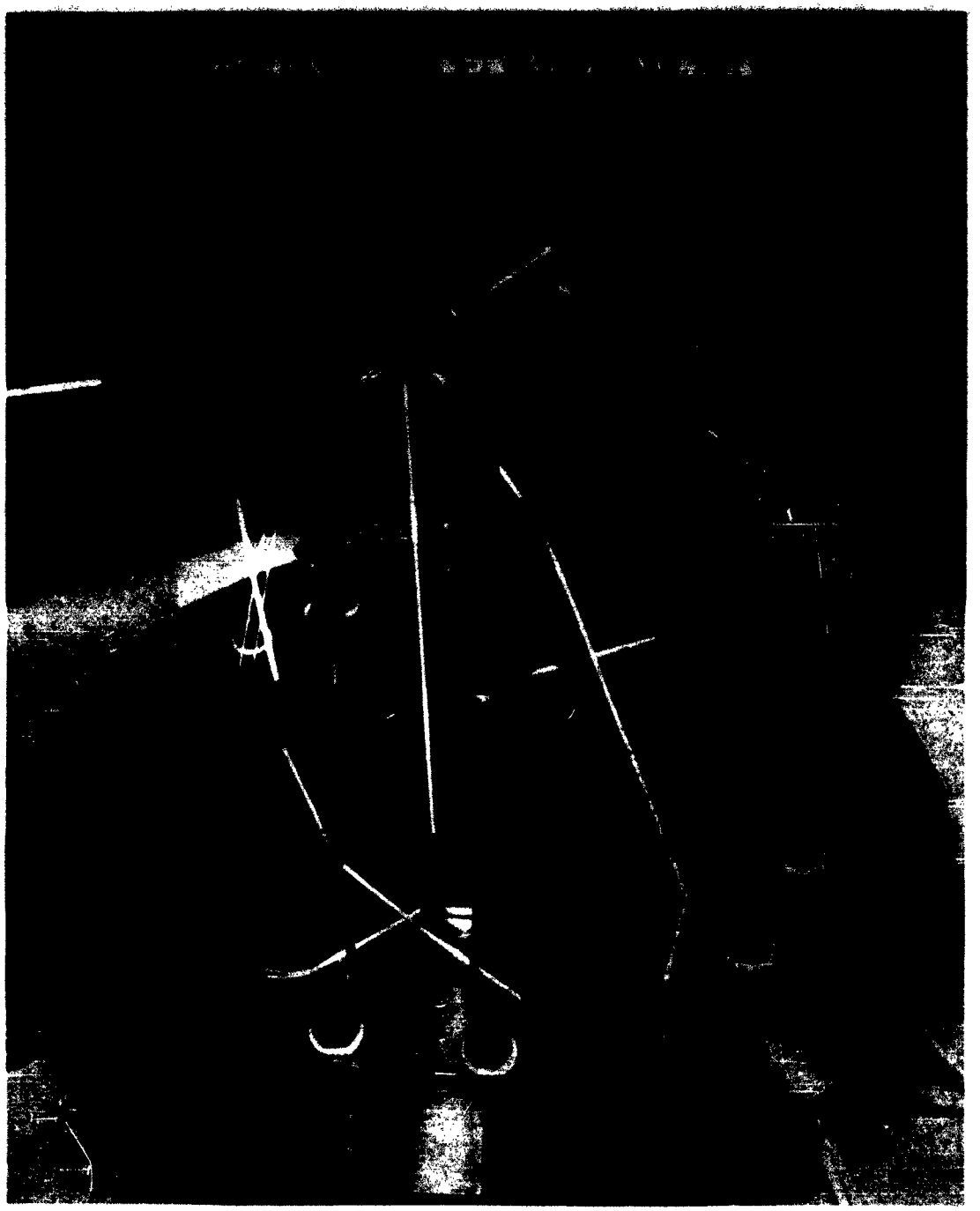

Figure 17. Converter B-1 Mounter for Test

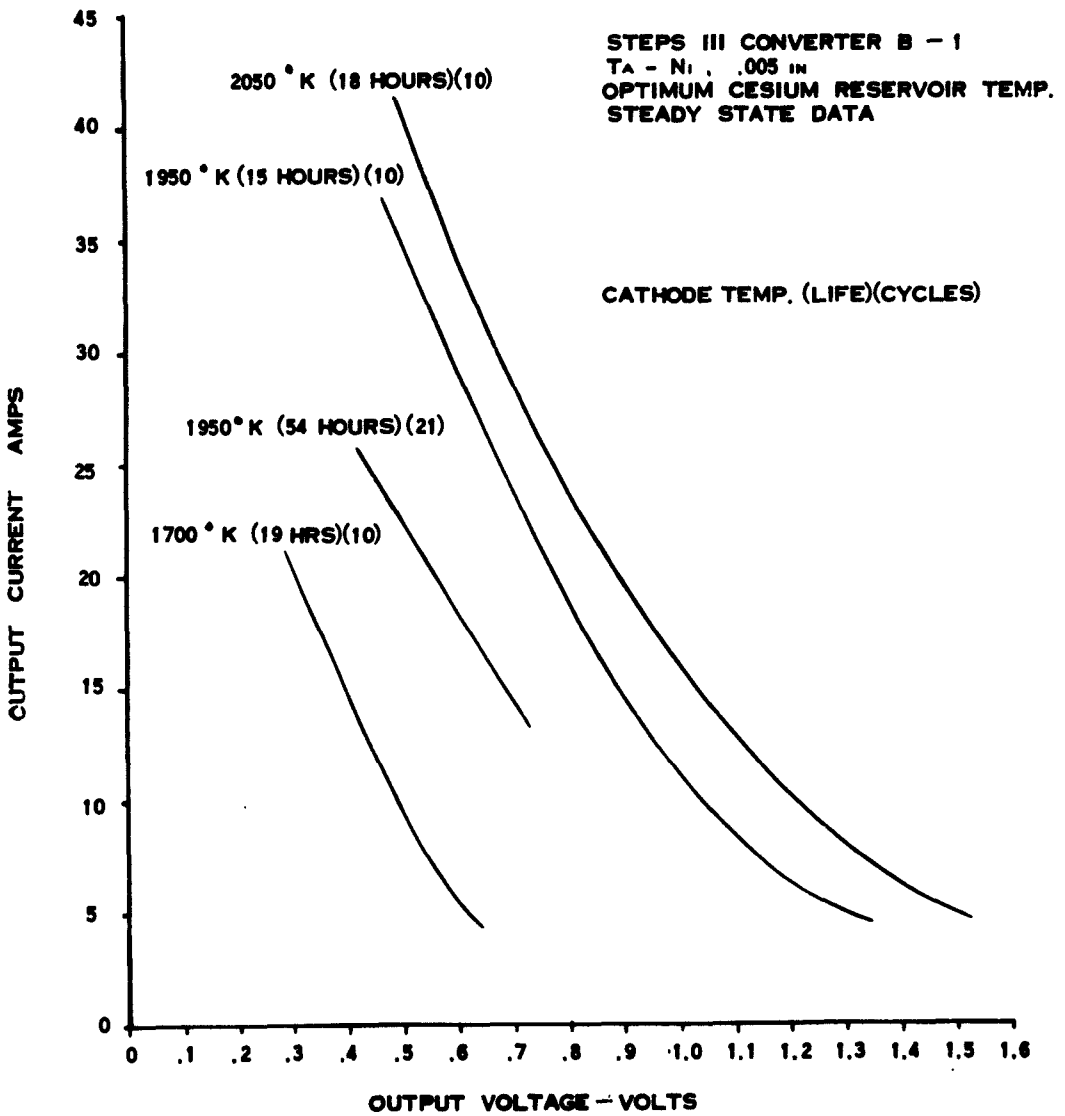

Figure 18. Converter B-1 E-I Characteristics

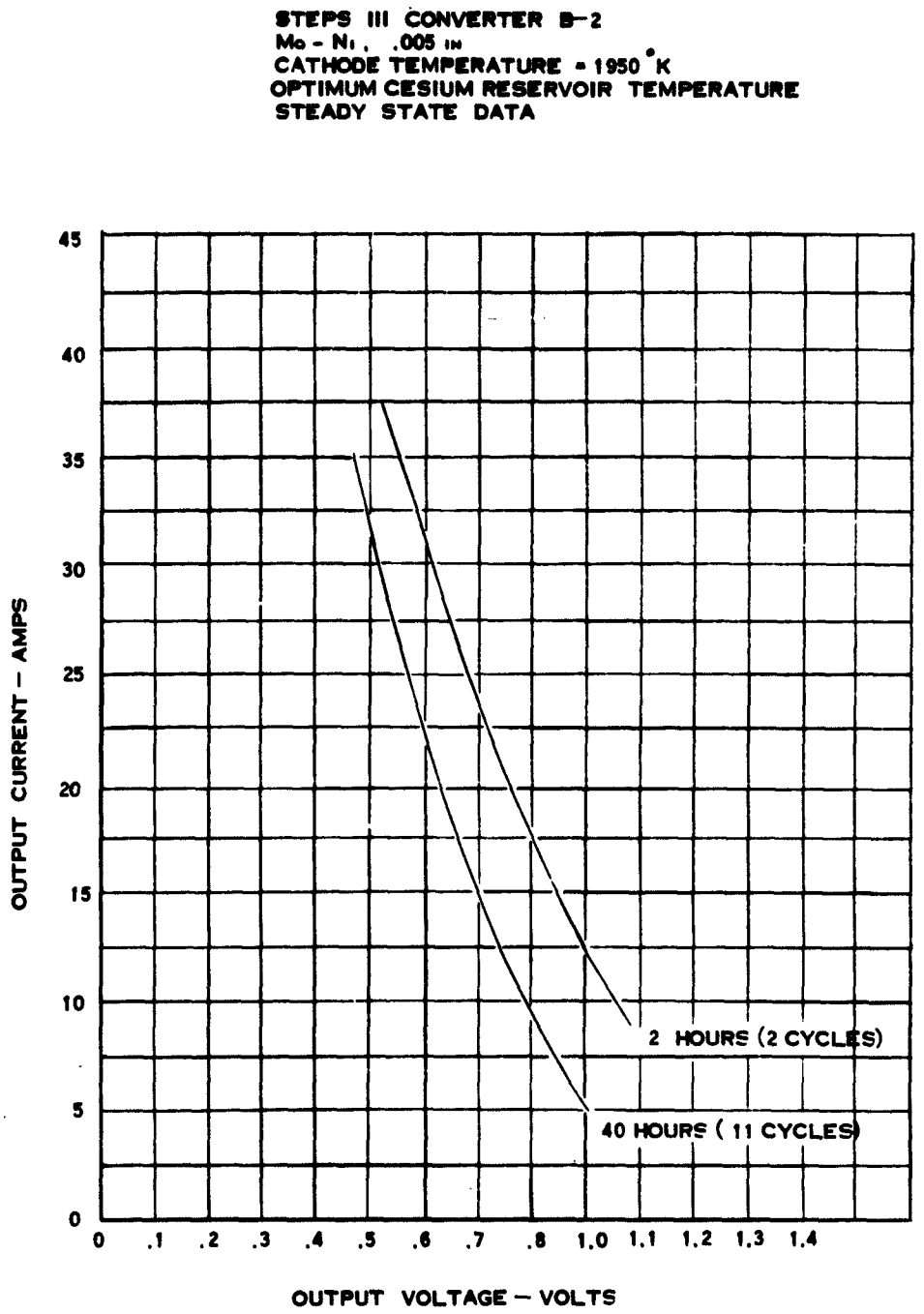

Figure 19. Converter B-2 E-I Characteristics

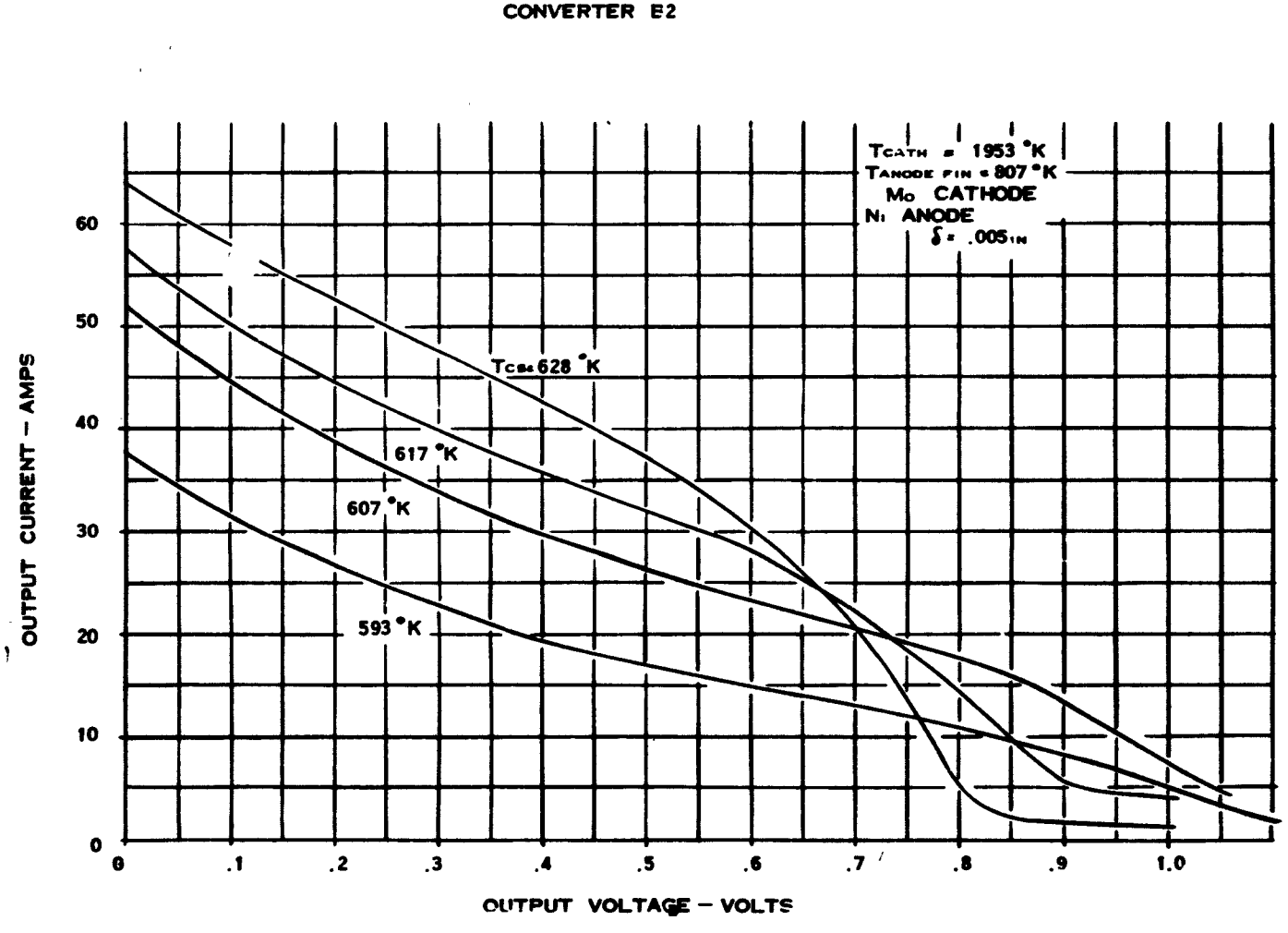

Figure 20. Converter B-2 1953°K E-I Characteristics at T_A = 807°K

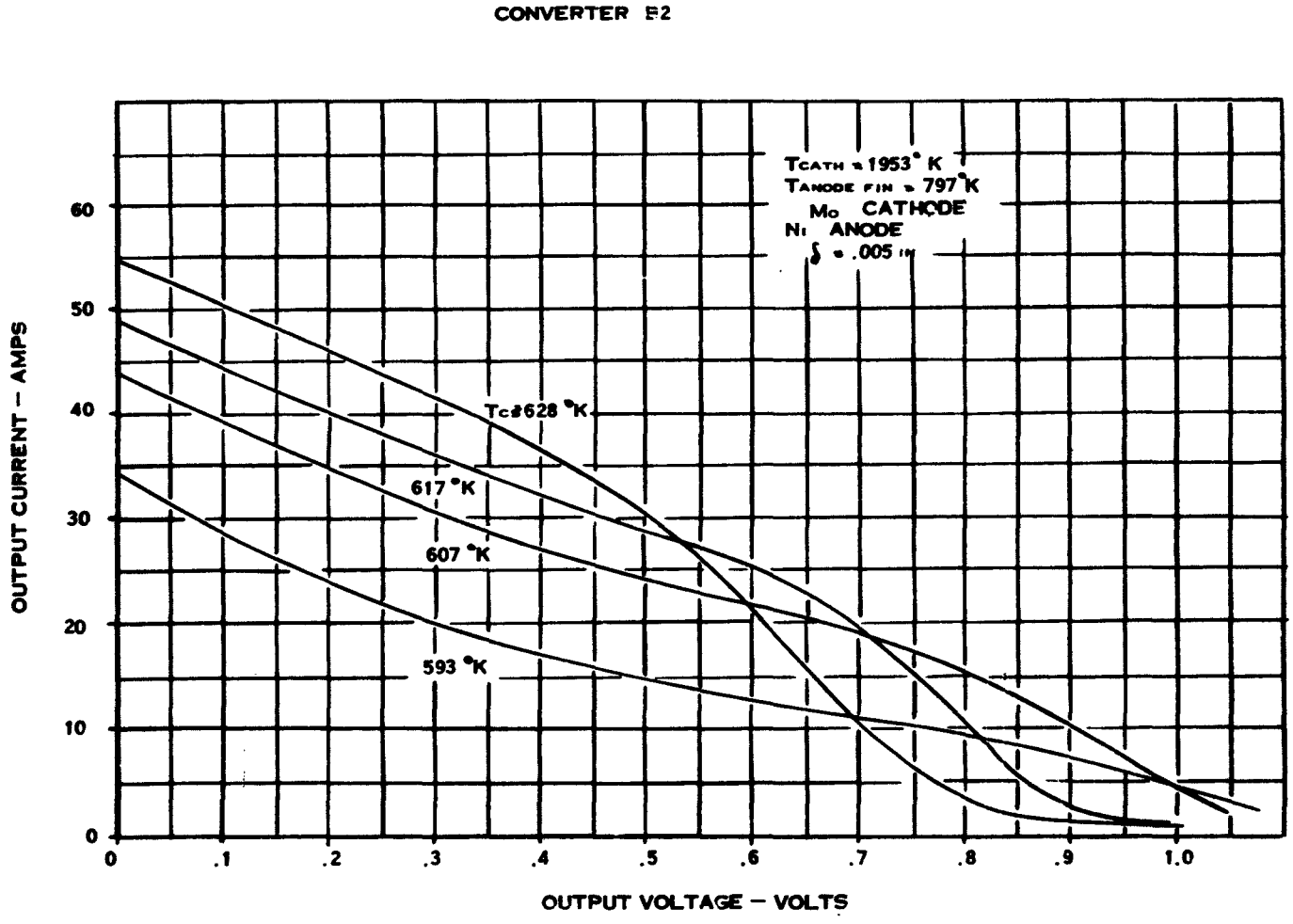

Figure 21. Converter B-2 1953°K E-I Characteristics at T_A = 797°K

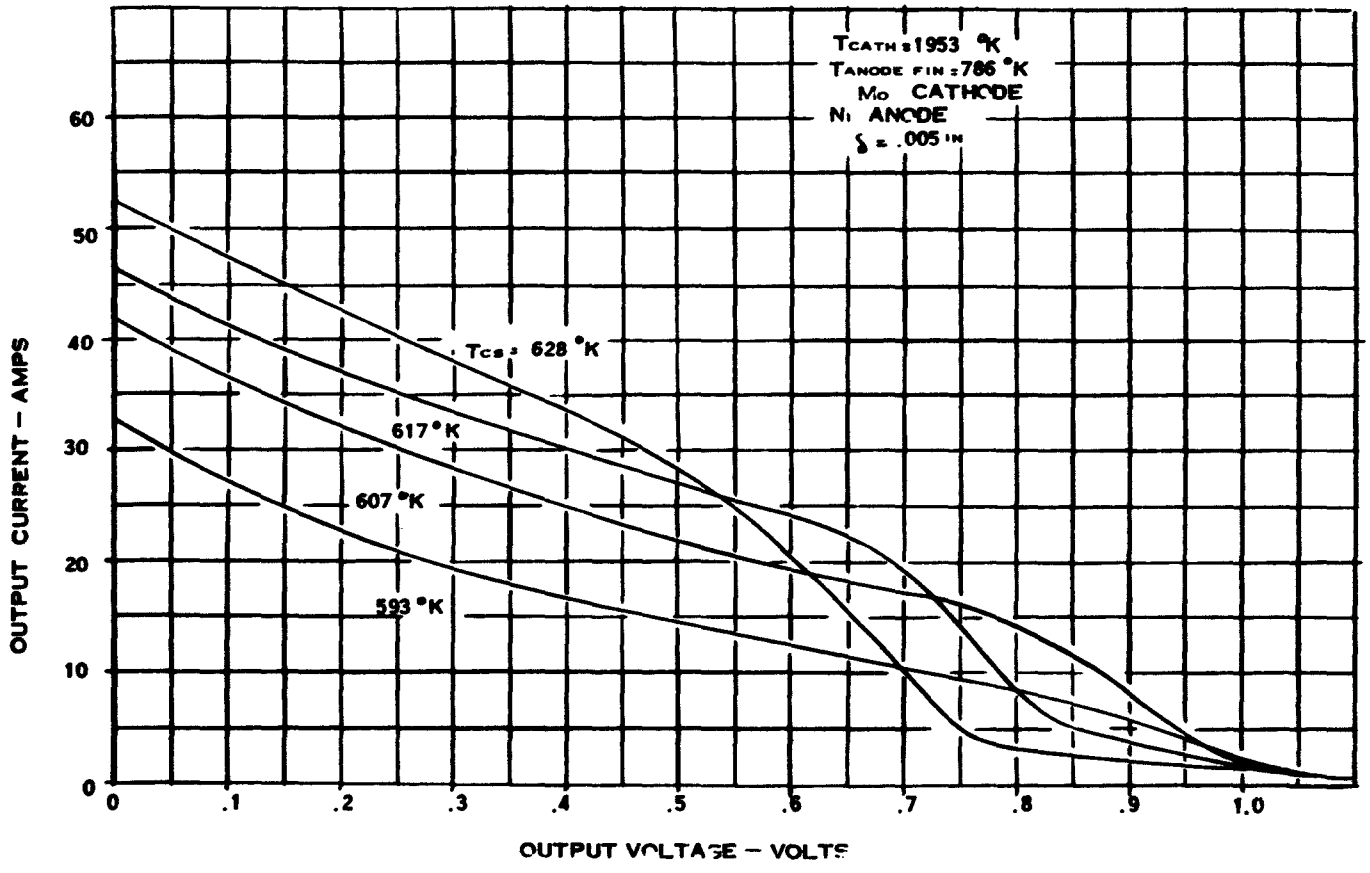

Figure 22. Converter B-2 1953°K E-I Characteristics at T_A = 786°K

CONVERTER B2

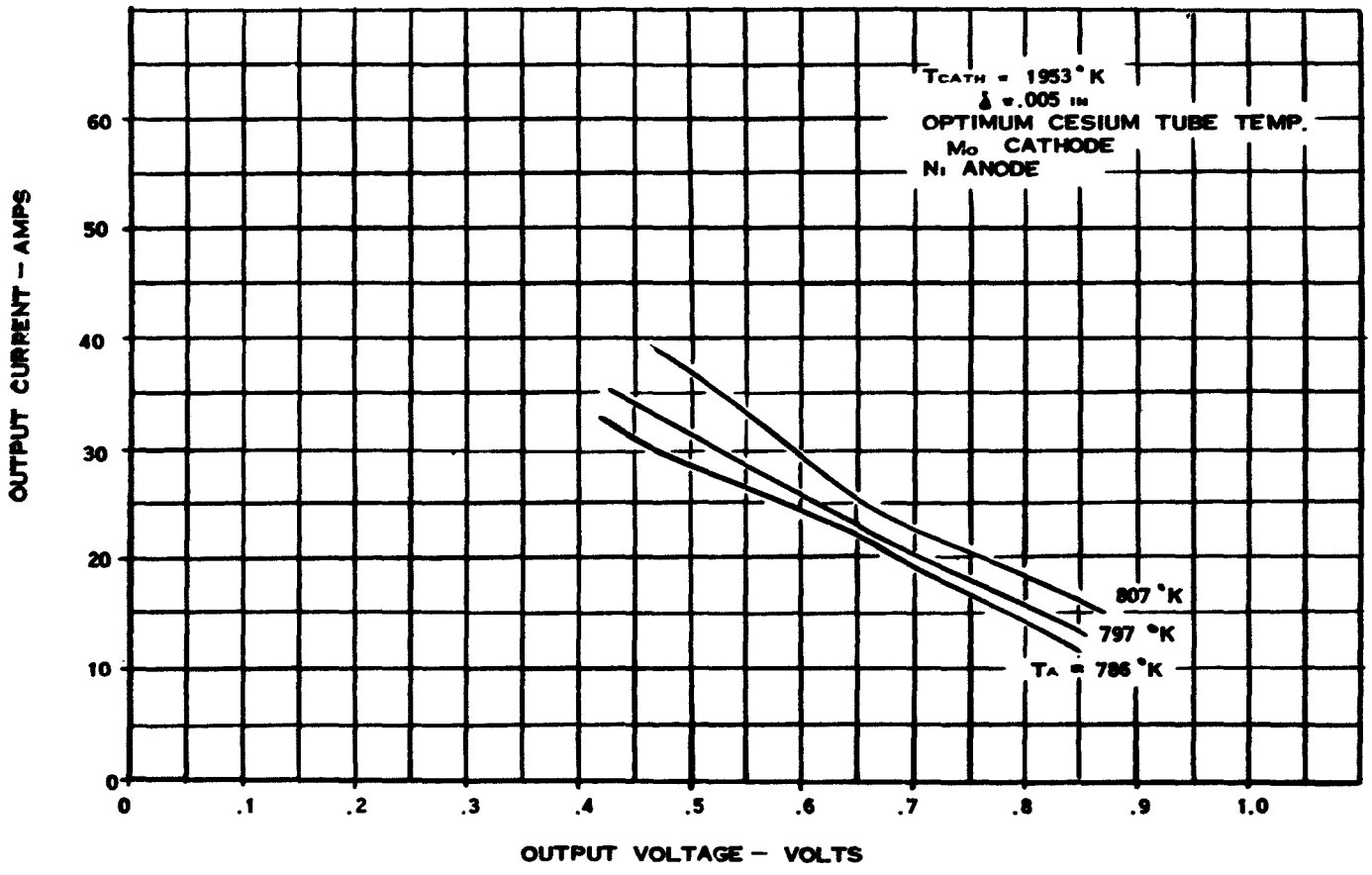

Figure 23. Converter B-2 1953°K E-I Characteristics at Optimum T_{cs}

CONVERTER B2

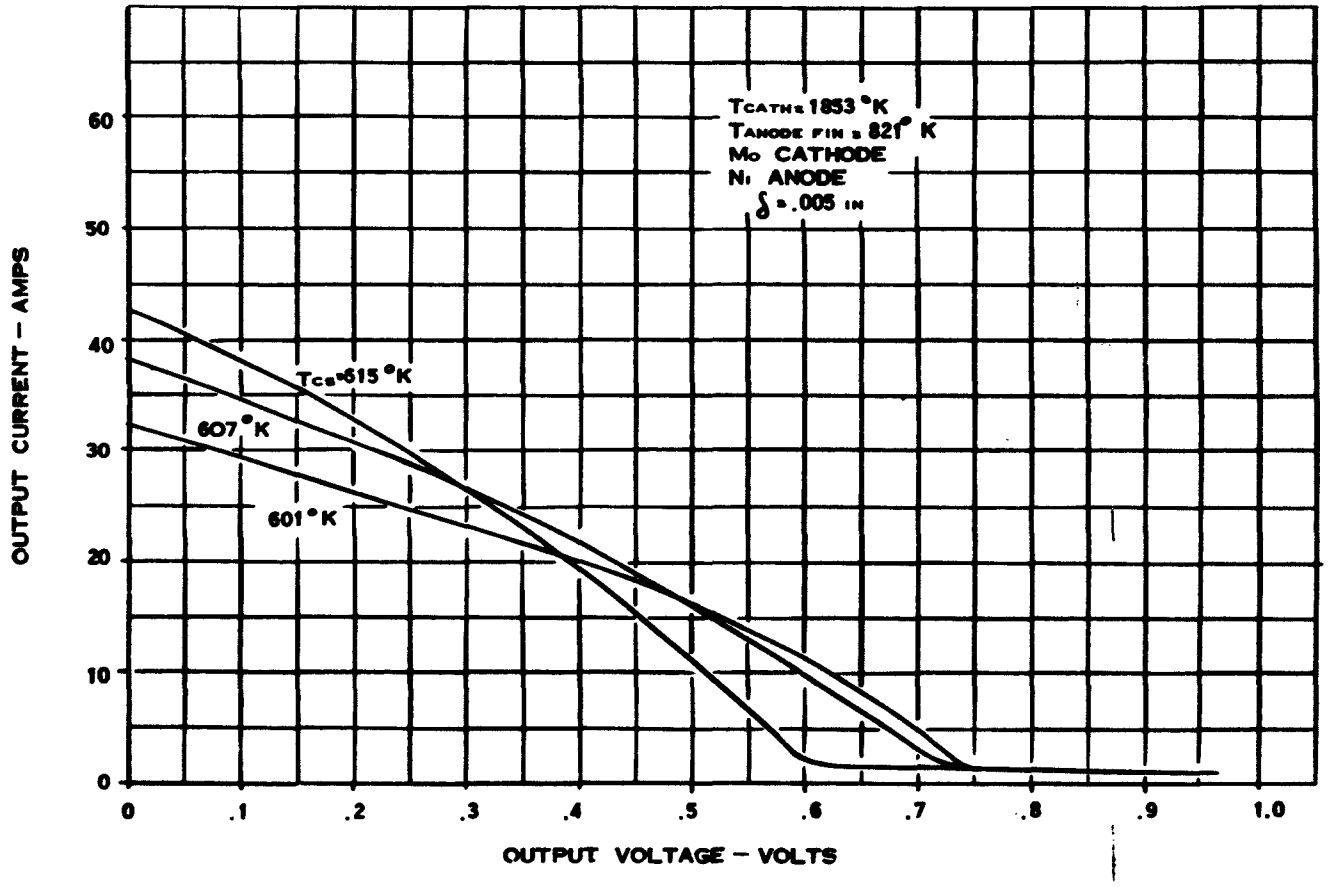

Figure 24. Converter B-2 1853°K E-I Characteristics at T_A = 821°K

CONVERTER B2

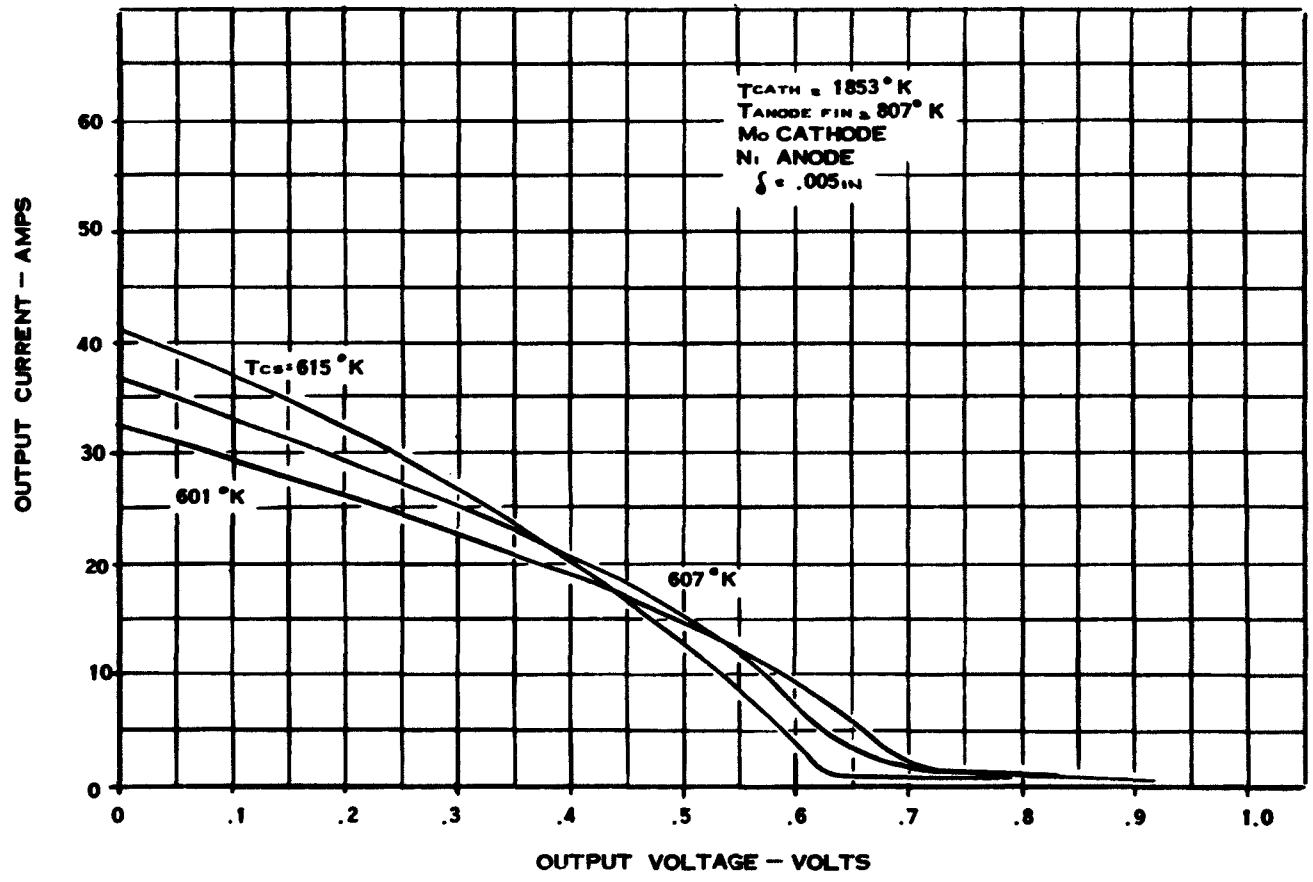

Figure 25. Converter B-2 1853°K E-I Characteristics at T_A = 807°K

CONVERTER B2

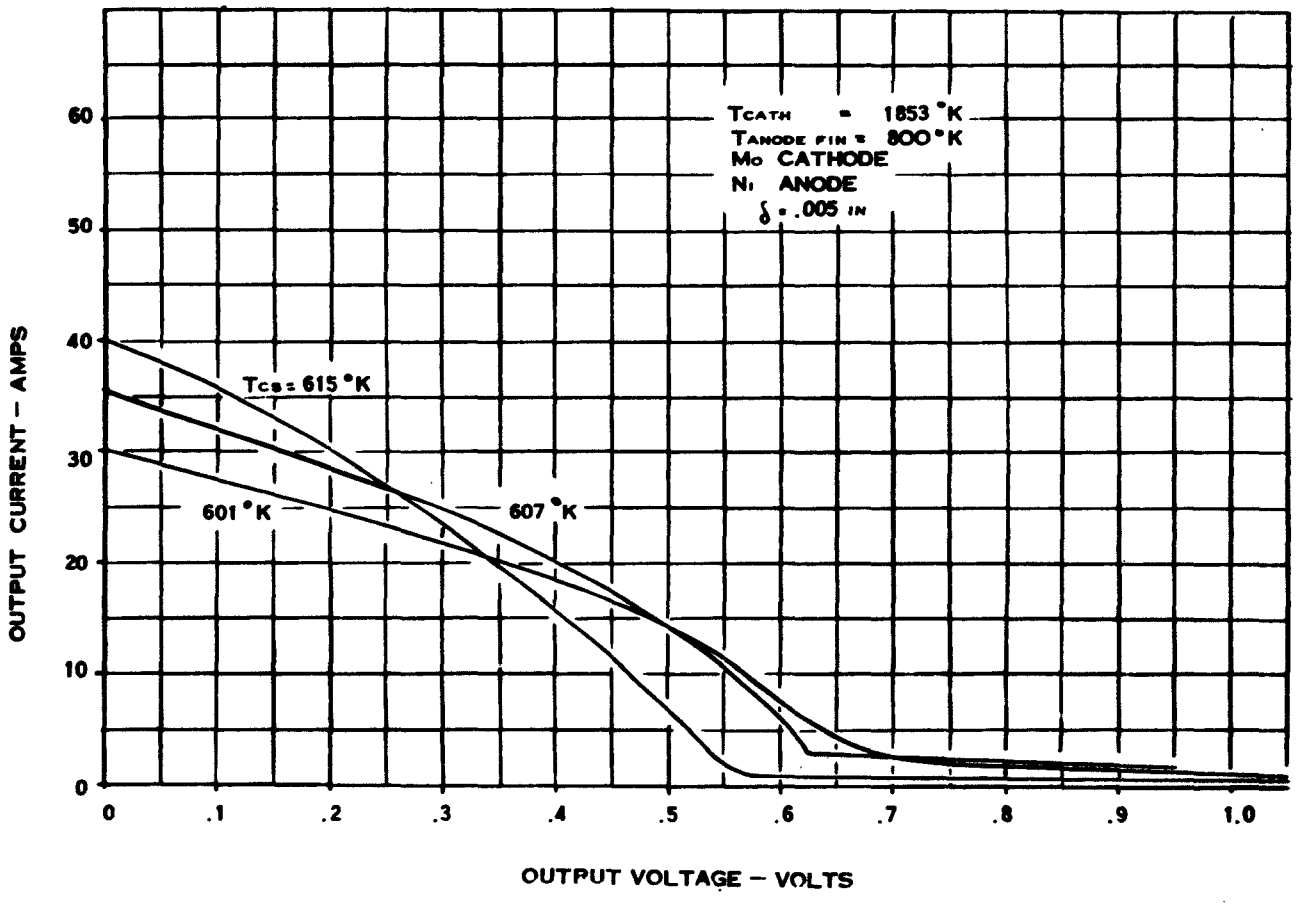

Figure 26. Converter B-2 1853°K E-I Characteristics at T_A = 800°K

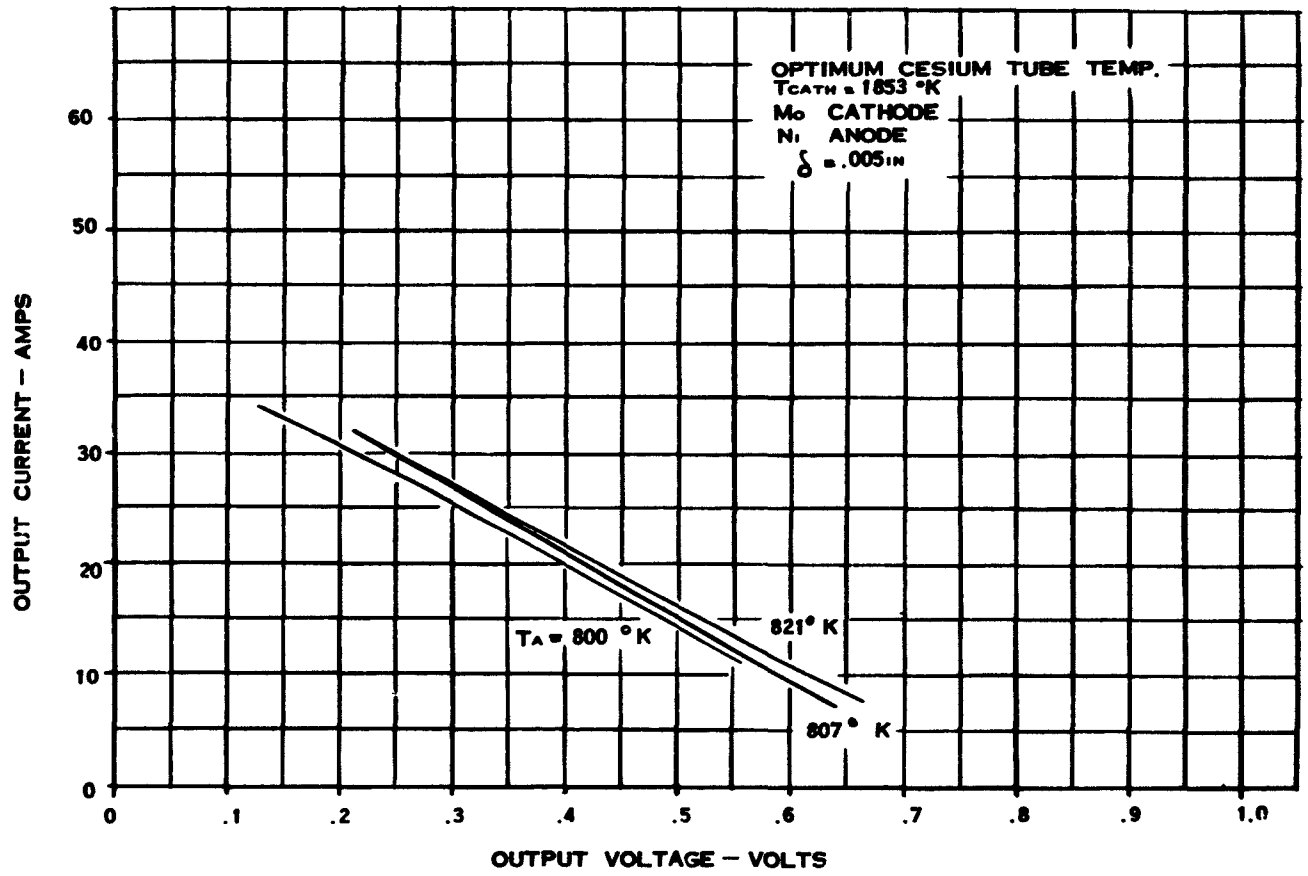

Figure 27. Converter B-2 1853°K E-I Characteristics at Optimum T_{cs}

REFERENCES

1. Advanced Solar Thermionic Generators, Quarterly Progress Report No. 1, Contract AF 33(657)-8947 by R.R. Herrick, R.C. Keyser, L.L. Dutram, December 1962.

2. Cavity Vapor Generator Final Report, ASD-TDR-62-899 by D.L. Purdy, R.C. Keyser, F.A. Blake and J.F. Williams, October 1962.

3. Design and Operation of Laboratory Type Parallel Plane Cesium Thermionic Converters, by V.C. Wilson and J. Lawrence in "Advanced Energy Conversion, Vol. 2, July/September 1962, p. 335-340, Pergamon Press.

4. Annual Technical Summary Report for the Thermionic Materials Research Program, by S.S. Kitrilakis, M.E. Meeker, and N.S. Razor, Report No. 2-63, Contract NONR-3563(00), 1962.

5. Thermal Conductance of Metallic Surfaces in Contact, H. French and W.M. Rohsenow; M.I.T. Heat Transfer Laboratory, Report #NYO-2136, May 1959.

6. Internal Design Consideration for Cavity-Type Solar Absorbers, by C.W. Stephens and A.M. Haire, ARS Journal, July 1961.

7. Radiant-Interchange Configuration Factors, by D.C. Hamilton and W.R. Morgan, NACA TN2836, December 1952.

8. DMIC Memorandum 141, 10 December 1961, Defense Metals Information Center, Battelle Memorial Institute, Columbus, Ohio.

DISTRIBUTION LIST

Copies	ACTIVITIES AT WPAFB
1	ASAPT
1	ASAPR
1	ASRMFP
3	ASRMFP-2 (A. E. Wallis)
1	ASRNET

OTHER DEPT OF DEFENSE ACTIVITIES

Navy

1 Office of Naval Research
Code 429
ATTN: Lt. Cmdr. John Connelly
Washington 25, D.C.

Air Force

1 AFCRL (CRZAP)
L. G. Hanscom Fld
Bedford, Mass.

1 AFOSR (SRHPM)
ATTN: Dr. Milton Slawsky
Bldg. T-D
Washington 25, D.C.

1 SSD (SSTRE)
ATTN: Capt. Evert
AF Unit Post Office
Los Angeles 45, California

24 ASTIA (TIPDR)
Arlington Hall Stn
Arlington 12, Va.

Copies	OTHER U.S. GOVT AGENCIES
1	U.S. Atomic Energy Commission Division of Reactor Development ATTN: Cmdr. W. Schoenfeld Washington 25, D.C.
1	Advanced Research Projects Agency ATTN: Dr. John Huth Washington 25, D.C.
1	Jet Propulsion Laboratory Spacecraft Secondary Power Section ATTN: Mr. Paul Goldsmith 4800 Oak Park Drive Pasadena, California
1	Aerospace Corporation ATTN: Library Technical Document Group Post Office Box 95085 Los Angeles 45, California
1	NASA - Lewis Research Center SEPO ATTN: Mr. R. Dennington 21000 Brookpark Road Cleveland 35, Ohio
1	U.S. Atomic Energy Commission San Francisco Operations Office ATTN: Reactor Division 2111 Bancroft Way Berkeley 4, California